

The Spectral Sequence from Khovanov Homology to Heegaard Floer Homology and Transverse Links

Author: Adam Saltz

Persistent link: <http://hdl.handle.net/2345/bc-ir:106790>

This work is posted on [eScholarship@BC](#),
Boston College University Libraries.

Boston College Electronic Thesis or Dissertation, 2016

Copyright is held by the author. This work is licensed under a Creative Commons Attribution-NoDerivatives 4.0 International License (<http://creativecommons.org/licenses/by-nd/4.0/>).

The Spectral Sequence from Khovanov
Homology to Heegaard Floer Homology
and Transverse Links

Adam Saltz

A dissertation submitted to the Faculty of the
department of Mathematics in partial fulfillment of the
requirements of the degree of Doctor of Philosophy.

Boston College
Morrissey College of Arts and Sciences
April 2016

© Copyright 2016 by Adam Saltz

The Spectral Sequence from Khovanov Homology to Heegaard Floer Homology and Transverse Links

Adam Saltz

Advisor: Professor John Arthur Baldwin, PhD

Abstract

Khovanov homology and Heegaard Floer homology have opened new horizons in knot theory and three-manifold topology, respectively. The two invariants have distinct origins, but the Khovanov homology of a link is related to the Heegaard Floer homology of its branched double cover by a spectral sequence constructed by Ozsváth and Szabó.

In this thesis, we construct an equivalent spectral sequence with a much more transparent connection to Khovanov homology. This is the first step towards proving Seed and Szabó's conjecture that Szabó's geometric spectral sequence is isomorphic to Ozsváth and Szabó's spectral sequence.

These spectral sequences connect information about contact structures contained in each invariant. We construct a braid conjugacy class invariant κ from Khovanov homology by adapting Floer-theoretic tools. There is a related transverse invariant which we conjecture to be effective. The conjugacy class invariant solves the word problem in the braid group among other applications. We have written a computer program to compute the invariant.

Contents

1	Topological preliminaries	7
1.1	Knots, links, and braids	7
1.1.1	Diagrams and invariants	7
1.1.2	Braids	9
1.2	Three-manifolds	11
1.2.1	Heegaard diagrams	13
1.2.2	Morse theory	13
1.2.3	Dehn surgery	15
1.3	Contact structures	16
1.3.1	Transverse links	17
2	Some homologies	21
2.1	Khovanov homology of links	21
2.1.1	Reduced Khovanov homology	24
2.1.2	Khovanov homology and transverse links	25
2.1.3	Khovanov homology and cobordisms	25
2.2	Heegaard Floer homology of three-manifolds	26
2.2.1	Formal properties	27
2.2.2	Definition	28
2.2.3	Computing Heegaard Floer homology	29
2.2.4	Two computations	31
2.2.5	Heegaard Floer homology and contact structures	32
2.3	The spectral sequence from $\widetilde{Kh}(L)$ to $\widehat{HF}(S^3(L))$	32
2.3.1	Why tho	32
2.3.2	Branched double covers and surgery	33
2.3.3	Pseudoholomorphic polygons	34
2.3.4	Bouquet diagrams	35
2.3.5	The connection between the transverse and contact invariants	40
3	Branched diagrams and the spectral sequence	41
3.1	Branched diagrams	42
3.2	Bouquet diagrams from branched diagrams	44
3.2.1	Admissibility and minimality	46
3.2.2	Correspondance with Khovanov chain complex	48
3.3	Handleslides	49
3.4	Comparison with Szabó's spectral sequence	54

4	An annular refinement of ψ	61
4.1	The annular filtration	64
4.2	Definition and invariance of κ	65
4.3	Examples and Properties of κ	66
4.3.1	Main example	66
4.3.2	Negative Stabilization	67
4.3.3	Positive Stabilization	67
4.3.4	Other properties and consequences	69
4.4	Invariants in reduced Khovanov homology	72

List of Figures

1	Two bowline knots. [19], [15]	1
2	These are diagrams of isotopic knots!	2
3		3
4	Curves on a torus.	4
1.1	Two diagrams of a trefoil knot.	7
1.2	The three Reidemeister moves. The moves only show a small part of a larger link diagram. The rest of the diagram is assumed to stay the same. The move can be understood as going from left to right or right to left. There are several variants of each move which are obviously also kosher, e.g. the twist in the first move could be made in the opposite direction.	8
1.3		9
1.4	The composition of the braid on the left with the braid on the right is the braid in Figure 1.3.	9
1.5	The Artin generator σ_2 in B_4 and its inverse σ_2^{-1} .	10
1.6	On the left, a genus 1 handlebody. On the right, a genus 2 handlebody.	12
2.1	The 0- and 1-resolution of a crossing.	22
2.2	From left to right: merge, split, cup, cap, and identity morphisms.	26
2.3		31
2.4		31
2.5	A schematic for the branched cover of S^3 over a trefoil knot.	33
2.6	A crossing and its two resolutions. One may realize the change of resolution from middle to right by a two-dimensional surgery along the dotted arc. Its image in the resulting diagram is also shown.	34
3.1	On the left, the 0-resolution of a crossing. In the middle, one side of the corresponding local picture on a branched diagram. On the right, the same for the 1 resolution. We have only shown one side of each branched diagram. The other side is identical.	43
3.2	A branched diagram from the $(1, 0, 0)$ resolution of a trefoil with the crossings ordered clockwise from the top left. The bar in the middle indicates that the two diagrams lie on different spheres, connected through the branch cuts. The left/top component is marked.	43
3.3	Three different local pictures of a branched multidiagram for a change of resolution. On the left, the local picture at the changed resolution. The other pictures are local pictures at unchanged crossings.	44

3.4	On top, both sides of $\mathcal{Bo}(I)$ at a 0-resolution. On the bottom, both sides of $\mathcal{Bo}(I)$ at a 1-resolution.	45
3.5	A bouquet diagram for the 0-resolution of an unknot. The lightly shaded region is the ‘obvious’ bigon for the left component. The darker region is topologically an annulus, but it can represent a holomorphic disk into the symmetric product of the Heegaard surface by cutting along a \mathbf{A} curve. . .	47
3.6	A branched multidiagram representing a handleslide at a 0-resolved crossing.	49
3.7	A holomorphic pentagon degenerates along a chord into a holomorphic triangle and rectangle. Supposing that the vertex v is where the green and purple edges meet, this degeneration is counted by $\psi_1 \circ D_0$	51
3.8	The \mathbf{B} curves for the paths $(0, \dots; 0) \rightarrow (1, \dots; 0) \rightarrow (1, \dots; 1)$ (left) and $(0, \dots; 0) \rightarrow (0, \dots; 1) \rightarrow (1, \dots; 1)$ (right). The intersection points constituting the highest degree generator are marked with circles. The shaded region is the region of the unique holomorphic triangle connecting the generators.	52
3.9	Configuration 2 in Szabó’s labeling.	56
3.10	Configuration 1 in Szabó’s labeling.	57
3.11	The branched Heegaard multidiagram from configuration 1. The black (resp. grey) dots mark intersection points which belong to the Heegaard Floer generators corresponding to $v_+ \otimes v_+$ on the starting (resp. ending) circles. . . .	58
3.12	A region corresponding to a Whitney quadrilateral. The orange regions have coefficient $+1$ and the negative regions have coefficient -1	59
4.1	Chain maps for positive stabilization	68
4.2	The result of the operation \vec{C}_p on two strands.	75
4.3	Values of $\underline{\kappa}_p$ and $\tilde{\kappa}_p$ may depend on p . The top braid is B_0 and the bottom braid is A_0 . The number above each arc represents a value of $\underline{\kappa}_p$ (for A_0) or $\tilde{\kappa}_p$ (for B_0) when p is placed on that arc.	76

Acknowledgments

I am particularly indebted to John Baldwin. John was a generous advisor who shared more ideas than I could digest and more time than he had. He corrected me without being dismissive and tolerated my trips down rabbit-holes without letting them go too far. I am lucky to have had him as an advisor. Thanks so much, John!

Eli Grigsby and Josh Greene, the other members of my committee, taught me a ton and were tremendously supportive. I learned lots of math and other important stuff from Ian Biringer, Martin Bridgeman, Marie Clote, Radu Cebanu, Neil Hoffman, Ben Howard, Rob Meyerhoff, Mark Reeder, and David Treumann. I am thankful to Marilyn Adams, Jo-Ann Bowen Cole, Sol Friedberg, Rob Meyerhoff for all they do for the department.

For many people, going to graduate school means moving somewhere unfamiliar without much social support. In Boston I was fortunate to already be a member of several incredible communities. I am grateful to all of you, old friends and new. Thanks in particular to my colleagues, the other students at Boston College.

Lastly, I am not exaggerating when I say that I cannot imagine having completed this degree – or doing much else – without the love and support of my family. Thank you.

In short, if you are reading this page because you thought “at least I’ll understand the acknowledgments,” then it’s likely that I am tremendously thankful for all your help and love.

Introduction

Knots, links, and braids are familiar to anyone who has owned a pair of shoes, watched the Olympics, or eaten challah. More than many other fields, knot theory offers the opportunity to translate concrete, ‘real-world’ ideas into formal mathematics. For example, compare the two knots in Figure 1. Any sailor worth her salt will tell you that these two are “the same knot” even though they are tied in different materials and the knot on the left is looser. This is very different from the concept of sameness usually found in a high school geometry class, where an 89° angle is never equivalent to a right angle, even though they are quite close. So we need a notion of equivalence for knots that is looser than equality. Two knots which are “the same” in the everyday sense are called *isotopic* in knot theory. Roughly, two knots are isotopic if one can be deformed to look like the other without any cutting. Such a deformation is called an *isotopy*.



Figure 1: Two bowline knots. [19], [15]

To do math on paper, we study knots through two-dimensional projections. But two diagrams for the same knot can look very different, see Figure 2. Translating facts about two-dimensional diagrams into facts about three-dimensional objects is a central technical concern in knot theory. Certain simple operations on a knot diagram produce another diagram for the same knot. Thanks to Reidemeister, we know a complete set of such moves: given one diagram for a knot, one can obtain any other by repeatedly applying three simple

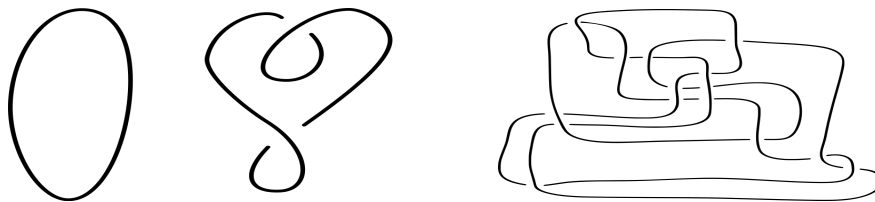


Figure 2: These are diagrams of isotopic knots!

moves. They are pictured in the next chapter, Figure 1.2. (Given two diagrams for the same knot, Reidemeister’s theorem does not say exactly how to transform one to the other, but just that some sequence of moves will do.)

Knots and links are only interesting insofar as they live in an ambient space. In contrast, the three-dimensional spaces we study are often lack a boundary or an embedding into an ambient space. We can’t pull our vision back to see the whole picture as we can with knots. It doesn’t make sense to talk about isotopy, because there is no ambient space in which to do the deformation. Instead, we talk about *diffeomorphic*¹ spaces; two spaces X and Y are diffeomorphic if there is a smooth function $f: X \rightarrow Y$ which has a smooth inverse. The map f is called a diffeomorphism. The diffeomorphism allows us to translate any topological statement about X into an equivalent statement for Y and vice-versa. One can say that X is the same space as Y but described differently, and f is a faithful and complete translation between the two descriptions.

All the spaces we study are *manifolds*, which means they look like ordinary Euclidean space close up. Three-dimensional Euclidean space, denoted by \mathbb{R}^3 , is a three-dimensional manifold. The three-sphere S^3 looks like \mathbb{R}^3 close up but has an extra point ‘at infinity’, just as the two-dimensional sphere can be seen as a disk (everything but the North Pole) with an extra point (the North Pole). A more exotic example is $S^1 \times S^2$, the three-dimensional space formed by attaching a two-dimensional sphere to every point of a circle.

Just like knots, three-dimensional spaces can be described by two-dimensional diagrams called *Heegaard diagrams*. There is a set of Reidemeister-type moves for these diagrams developed by Reidemeister and Singer. The basic idea behind Heegaard diagrams is to

¹We will also sometimes use the terms *homeomorphic* and *homeomorphism*, which use *continuous* maps rather than smooth maps. This is a purely technical concern for one-, two-, and three-dimensional spaces. In four dimensions the difference is quite important and interesting in general, but we won’t need to think much about it.



Figure 3

divide a three-dimensional space into two simple pieces separated by a surface. Because the pieces are so simple, all of the complexity of the space is encoded by the way the pieces are attached to the surface. This attachment can be described by drawing curves on a surface, and a picture of these curves is a Heegaard diagram.

Knot theory and the study of three-manifolds are closely related. For one, there is an operation called surgery along a knot or link which transforms one manifold into another. This operation is so powerful that it can transform the three-sphere, the simplest three-manifold, into any other three-dimensional manifold. One can gain insight into a three-manifold by studying the surgeries which create it and vice-versa. Second, for every link in the three-sphere there is a special three-manifold called its branched double cover. It has long been recognized that the manifold-theoretic properties of branched covers reflect the knot-theoretic properties of the underlying link, and vice-versa.

The connection between the two subjects persists in more recent developments. Low-dimensional topology has been lit up by two new tools, *Khovanov homology* for links and *Heegaard Floer homology* for three-manifolds. These two are connected through the double branched cover construction. This connection is central to all the work in this thesis, whose central motivation is that if we see something interesting in one theory, we should go looking for it in the other.

We can illustrate the basic idea of homology by thinking about intersections between curves. We're supposed to be able to wiggle things around in topology, so the two pictures in Figure 3 should be thought of as equivalent. The two intersection points in Figure 3b are not essential, in the sense that you could remove them by wiggling. On the other hand, in Figure 4, we see two curves on a torus with an intersection point which cannot be wiggled away (try it!). So to understand intersections from a topological perspective, we need to do more than count intersection points. We need to record the relationships between them, and we need to analyze these relationships to identify which points are important and which

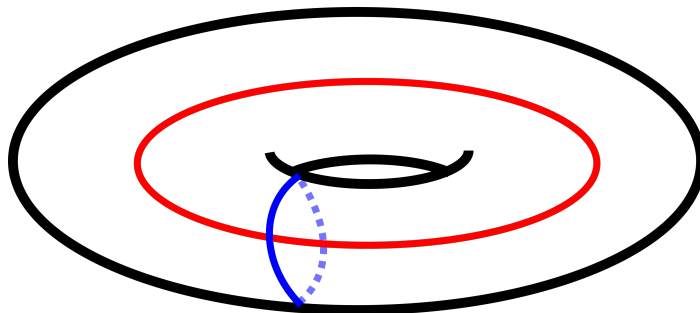


Figure 4: Curves on a torus.

aren't.²

The mathematical object which encodes all this information is necessarily more complicated than a number or even a list of numbers. It's called a *chain complex* which is *generated* by the intersection points. The gadget which records relationships between intersection points is a function on the chain complex called a *differential*, and the simplified structure containing only essential information is called the *homology* of the chain complex. The configurations of curves in Figure 3 will yield different chain complexes (because they have different numbers of intersection points) but the same homology.

Heegaard Floer homology is a tool for studying three-dimensional manifolds defined by Ozsváth and Szabó. Let Y stand for a three-manifold. Pick any³ Heegaard diagram which represents Y . The Heegaard Floer chain complex is generated by certain families of intersection points between the curves in the diagram. It takes a lot of work to even define the differential, which comes from symplectic geometry. A foundational theorem, proved by Ozsváth and Szabó, states that the homology of this chain complex will be the same no matter which diagram for Y you start with. Heegaard Floer homology has been used to prove all sorts of theorems about three-manifolds, often by choosing a diagram adapted to a particular problem.

Khovanov homology is a tool for studying knots and links defined by Khovanov. Khovanov was motivated, in part, by the *Jones polynomial*, an easy to define but mysterious

²In fact, the idea of essential versus inessential points is somewhat misleading. In other contexts, we can find curves which intersect three times with only one essential intersection. But the points are all on equal footing: one cannot say that one is more essential than the other. Rather, we can only say that among the three of them, one is essential and the other two are redundant. We say that the three points are *homologous*, that they together form a *homology class*, and that any one of them is a *representative* of the class.

³Well, not any.

gadget developed by Jones in the 1980s. Let K stand for a link, and pick any diagram for K . Jones constructed an algorithm for producing a polynomial from the diagram, and he showed that the polynomial does not depend on your choice of diagram for K .⁴ Just as the homology we first described provides a richer picture of intersection numbers, Khovanov homology provides a richer picture of the Jones polynomial.

Khovanov and Heegaard Floer homology were developed in the same period, and it was quickly realized that the Khovanov homology of a link should be related to the Heegaard Floer homology of its branched double cover. Ozsváth and Szabó constructed such a relation in the form of an algebraic gadget called a *spectral sequence*. Concretely, this is an algorithm for computing the Heegaard Floer homology of the branched double cover of a link which, as an intermediate step, computes the Khovanov homology of that link. And this is not just any algorithm: it starts with a large chain complex and computes the homology of the whole thing by computing the homology of smaller pieces, one at a time. The result at each step is simpler than at the previous step. This implies that the Heegaard Floer homology of a link's branched double cover is simpler than that link's Khovanov homology. This is a striking result given the very different origins of Heegaard Floer homology and Khovanov homology.

The first piece of original work in this thesis is an alternative construction of this connection. Ozsváth and Szabó use complex Heegaard diagrams to construct their spectral sequence. We show that an equivalent spectral sequence can be built from simpler Heegaard diagrams with a much more transparent connection to Khovanov homology. In a certain sense, these are the simplest possible Heegaard diagrams one could use; if they were any simpler, they could not encode Khovanov homology. It is easy to use these diagrams to see how the spectral sequence translates certain pieces of Khovanov-theoretic data into Floer-theoretic data.

Szabó constructed another spectral sequence which he and Seed conjectured to be equivalent to Ozsváth and Szabó's. The Szabó spectral sequence is much easier to work with. Our original motivation for this work was to prove the conjecture using our diagrams as a

⁴For example, the Jones polynomial of square knot is $(q^{-1} + q^{-3} - q^{-4})(q + q^3 - q^4)$, and the Jones polynomial of an unknotted circle is 1. It is not known if any other knot has Jones polynomial 1!

bridge between the two theories. Unfortunately, our spectral sequence is provably not the same as Szabó's. Nevertheless, the differences between the two theories are quite interesting, and we hope to revisit the problem in future work. This work previously appeared in our note "Branched diagrams and the Ozsváth-Szabó spectral sequence", available on the Arxiv [57].

In the next chapter, we construct a new tool for studying transverse links using Khovanov homology. Although this chapter does not use Floer homology, the motivation came from the Ozsváth-Szabó spectral sequence. Various Heegaard Floer enthusiasts, inspired by work of Hutchings, Latschev, and Wendl, have tried to use Heegaard Floer homology to give more sensitive information about contact structures (an interesting three-dimensional thing) than had previous been possible. Baldwin suggested that we look for an equivalent structure in Khovanov homology. Our tool, called κ , assigns to each braid a positive, even number. If two braids are equivalent in a certain way, they must have the same value of κ . By studying how κ changes for different braids, we are able to answer braid-theoretic questions. We also disprove a conjecture about an elaboration of Khovanov homology called annular Khovanov homology. The contents of this chapter are joint work with Diana Hubbard, and appeared in our article "An annular refinement of the transverse element in Khovanov homology" [29].

We have tried to keep the first chapter readable by non-mathematicians, but there are some places where we cannot avoid a technical viewpoint. We abandon that effort in all the following chapters.

To recap: in Chapter 1, we review the basic topological constructions which are essential to what follows. In Chapter 2, we review Khovanov homology and Heegaard Floer homology. In Chapter 3, we construct a simplification of the Ozsváth-Szabó spectral sequence. In Chapter 4, we define a conjugacy class invariant of braids which we use to study transverse links and certain spectral sequences.

Chapter 1

Topological preliminaries

The fundamental objects of study in low-dimensional topology are knots, surfaces, and three- and four-dimensional manifolds. In this chapter we review the facts and constructions about these objects which will be fundamental to the rest of the thesis.

1.1 Knots, links, and braids

1.1.1 Diagrams and invariants

A *knot* is a smooth embedding of a circle into three-sphere S^3 , or, almost equivalently, three-dimensional Euclidean space \mathbb{R}^3 . A *link* is a smooth embedding of several circles into S^3 (or \mathbb{R}^3). We often study links by studying their projections to a plane. Usually, such a projection has points where two or more strands overlap. We may assume that at most two strands overlap at any single point. Such a projection along with the information of which strand crosses over which at double points is called a *diagram*. See Figure 1.1.

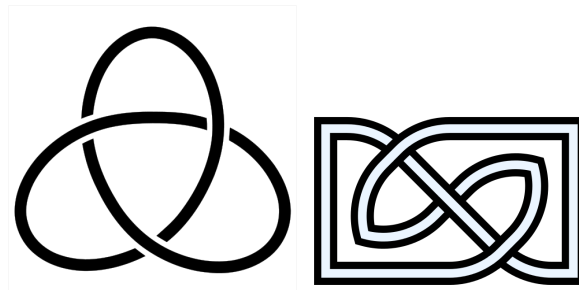


Figure 1.1: Two diagrams of a trefoil knot.

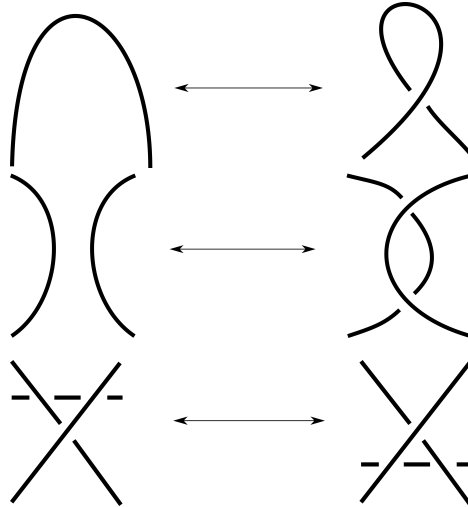


Figure 1.2: The three Reidemeister moves. The moves only show a small part of a larger link diagram. The rest of the diagram is assumed to stay the same. The move can be understood as going from left to right or right to left. There are several variants of each move which are obviously also kosher, e.g. the twist in the first move could be made in the opposite direction.

Anyone who has played Cat’s Cradle knows that a link has many diagrams. It is important to understand how different diagrams for the same link are related – after all, we are ultimately interested in knots and links rather than diagrams. Certainly, one is free to push around the curves in a diagram without creating or destroying any crossings. This operation is called *planar isotopy*. A complete characterization of how diagrams for the same knot may be related was first provided by Reidemeister in 1926.

Theorem. [56] *Any two diagrams for a link are related by a finite sequence of planar isotopies and the three moves shown in Figure 1.2.*

This theorem allows us to distinguish between properties of link and properties of their diagrams. For example, as the first and second Reidemeister moves change the number of crossings in a diagram, “number of crossings” is a property of diagrams rather than of links.¹ On the other hand, every diagram for a particular link will always have the same number of components. Thus “number of components” is a property of a link which can be computed from any diagram. Properties of links which can be computed from a diagram

¹One way to address this issue is to define the *crossing number* of a link as the minimum number of crossings in all diagrams for that link. This fix – taking the minimum or maximum over all diagrams – tends to produce knot invariants which can only be computed using cleverness, as the set of all diagrams for a link is infinite. See Section 4.3 for an example.

are called *link invariants*.²

1.1.2 Braids

A braid is a set of strands as in Figure 1.3. The strands are not permitted to backtrack, and there can be no closed circles. Just as with knots, we will consider two braids to be the same if one can be isotoped to the other. The number of endpoints on either end of a braid is called its *index*.



Figure 1.3

Two braids with the same index may be *composed* by stacking one on top of the other. For braids β and β' with the same number of endpoints, write $\beta\beta'$ for their composition. For every index there is an *identity braid* 1 which consists of only vertical strands. It is clear that $\beta 1 = 1\beta = \beta$. Every braid β has a unique *inverse* β^{-1} so that $\beta\beta^{-1} = \beta^{-1}\beta = 1$. The group of braids with n strands is called the *n -strand braid group* and is denoted B_n .

Artin [3] discovered a useful, purely algebraic presentation of the braid group. Let $\sigma_i \in B_n$ be the braid in which the $(i+1)$ -st strand crosses over the i -th strand and all other strands are vertical. See 1.5.

²The term “link invariant” is often used to describe any old property of a link. For example, the crossing number cannot in general be computed from a single link diagram, and it is not clear to the author in what sense it is “invariant.”

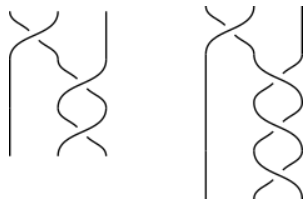


Figure 1.4: The composition of the braid on the left with the braid on the right is the braid in Figure 1.3.

Theorem. *The braid group B_n is generated by³ $\sigma_1, \dots, \sigma_{n-1}$ subject to the following relations:*

- *If $|i - j| > 1$, then $\sigma_i \sigma_j = \sigma_j \sigma_i$.*
- *If $|i - j| = 1$, then $\sigma_i \sigma_j \sigma_i = \sigma_j \sigma_i \sigma_j$.*

It is easy to convince oneself that the σ_i generate B_n and to prove the relations by drawing a picture or three. The question of whether two sequences of generators represent the same element in B_n is called *the word problem*. There are several available solutions to the braid group, e.g. by Artin [3] and Garside [21]. We provide another in Corollary 4.3.7, section 4.3.



Figure 1.5: The Artin generator σ_2 in B_4 and its inverse σ_2^{-1} .

A braid can be closed into a link by connecting the top endpoints to the corresponding bottom endpoints. We write $\hat{\beta}$ for the closure of β . We will call a diagram \mathcal{D} a *braid closure diagram* if there is some β so that \mathcal{D} is planar isotopic to $\hat{\beta}$.

Proposition. *(Alexander, [1]) Every link is the closure of a braid.*

Markov [42] characterized precisely when two braids close to isotopic links. Before we can state his theorem, we need to define two additional operations on braids. First, let σ be a braid on n strands. There is a map $c_\sigma: B_n \rightarrow B_n$ defined by $c_\sigma(\beta) = \sigma^{-1}\beta\sigma$ called *conjugation* by σ . Second, there is a pair of maps $S^\pm: B_n \rightarrow B_{n+1}$ defined by $S^\pm(\beta) = \beta\sigma_n^{\pm 1}$. These operations are called *positive and negative stabilization*. Conjugation and stabilization are together called *Markov moves*. Applying a Markov move to a braid β certainly alters β , but it does not alter $\hat{\beta}$ (try it!).

Theorem. *Two braids close to isotopic links if and only if they are related by a finite sequence of Markov moves.*

³i.e. “every braid may be written as a composition of”

The n -strand braid group may also be understood as the *mapping class group* of a disk with n marked points. The mapping class group of a manifold with marked points is set of diffeomorphisms of that manifold modulo⁴ those diffeomorphisms which are isotopic to the identity and with the proviso that diffeomorphisms may permute the marked points. We think of the braid as a distortion of the disk which braids the marked points. One can keep track of this action through certain arcs on the punctured disk, as follows. The following two definitions (with more detail) can be found in [7]. Let D_n denote the standard unit disk in \mathbb{C} with n marked points p_1, \dots, p_n positioned along the real axis.

Definition. An arc $\gamma: [0, 1] \rightarrow D_n$ is admissible if it satisfies

1. γ is a smooth embedding transverse to ∂D_n
2. $\gamma(0) = -1 \in \mathbb{C}$ and $\gamma(1) \in \{p_1, \dots, p_n\}$
3. $\gamma(t) \in D_n - (\partial D_n \cup \{p_1, \dots, p_n\})$ for all $t \in (0, 1)$ and
4. $\frac{d\gamma}{dt} \neq 0$ for all $t \in [0, 1]$.

Definition. The braid $\sigma \in B_n$ is *right-veering* if for all admissible arcs γ , the arc $\sigma(\gamma)$ lies to the right of γ when pulled tight.

A negatively stabilized braid is not right-veering. and neither is a σ_i -*negative* braid is not right-veering. (σ_i -negative means that the braid can be represented by a word which contains σ_i^{-1} but not σ_i for some i .)

1.2 Three-manifolds

A manifold is a topological space which looks Euclidean close up. For example, the piece of Earth within the reader's field of vision⁵ is essentially Euclidean despite the fact that the Earth is widely believed to be round [2]. So the surface of the Earth can be modeled as a *two-dimensional manifold* because up close it looks like two-dimensional Euclidean space.

In this thesis, we study three- and four-dimensional manifolds. *Heegaard diagrams* are an essential tool to visualize these spaces, so we introduce them next. After that we touch

⁴i.e. "in which we declare to be equal"

⁵Here we exclude exceptionally tall or airborne readers.

briefly on Morse theory, which offers a proof that every three-manifold has a Heegaard diagram and motivates the construction of Heegaard Floer homology in Section 2.2. Next we define the essential operation of Dehn surgery. These two sections are rather technical. We end the chapter with a discussion of contact structures and transverse links in three-manifolds.

All the three-manifolds in this paper may be assumed to be closed, connected, and orientable unless otherwise noted.

Before proceeding, we introduce two essential building blocks of manifolds. First, a n -dimensional k -handle is an n -dimensional ball with a special decomposition of its boundary. More precisely, an n -dimensional k -handle is the space $\mathbb{R}^k \times \mathbb{R}^{n-k}$ with boundary $\mathbb{R}^{k-1} \times \mathbb{R}^{n-k} \cup \mathbb{R}^k \times \mathbb{R}^{n-k-1}$. The first component of the boundary is called the *attaching disk* and the second is called the *co-attaching disk*. To *attach* a handle to a manifold, one identifies a neighborhood of the attaching disk of the handle with some disk on the base manifold. A *handle decomposition* of a manifold is a sequence of handle attachments which produce the manifold.

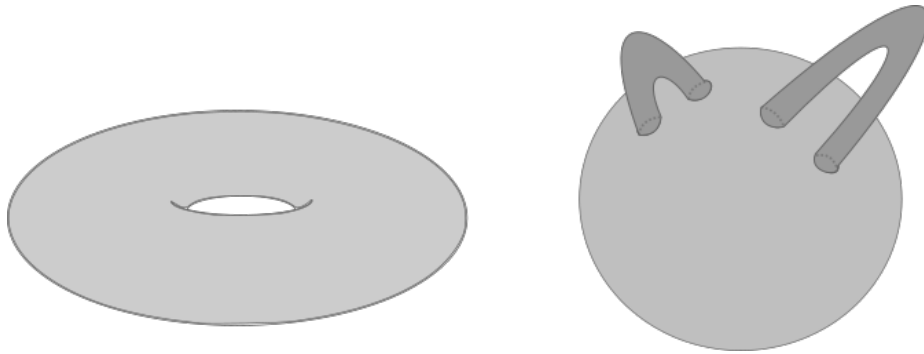


Figure 1.6: On the left, a genus 1 handlebody. On the right, a genus 2 handlebody.

Second, an n -dimensional *handlebody* is an n -dimensional space which retracts to a wedge of circles, see Figure 1.6. In dimension three, the *genus* of a handlebody is the genus of its boundary, i.e. the number of holes in the surface. Three-dimensional handlebodies are classified up to diffeomorphism by their genus.

1.2.1 Heegaard diagrams

Let Y be a three-manifold and $\Sigma \subset Y$ a closed, oriented surface. The pair (Y, Σ) is called a *Heegaard splitting* if Σ divides Y into two parts, each of which is diffeomorphic to a handlebody. For example, if one visualizes S^3 as \mathbb{R}^3 with an extra point, the unit sphere around the origin splits S^3 into two three-dimensional balls. The standard torus splits S^3 into two solid tori, and so on.

Let us consider the reverse perspective. Let Σ be a genus g , compact, oriented surface. If we attach g 1-handles to the inside so that they do not overlap, the resulting boundary (on the inside) is a sphere, which can be filled in by a ball in exactly one way. The space is now a handlebody. On the outside of this surface, we may draw the co-attaching circles of g 2-handles. After attaching the 2-handles, the remaining boundary component is again a sphere, and by filling it in we obtain a closed three-manifold. The upshot is that a genus g handlebody, along with two sets of g curves (satisfying some technical conditions), describe two handlebodies glued along a common boundary.

Definition. A *Heegaard diagram* is a genus g surface along with two sets of g homologically independent curves.

Every three-manifold may be described by a Heegaard diagram. Figure 4 (from the introduction) and Figure 2.3 is a Heegaard diagram from S^3 . Figure 2.4 is a diagram for $S^1 \times S^2$. The curves can also twist around the torus in more complicated ways, in which case the diagram represents a *lens space*. A Heegaard diagram for a more complicated three-manifold must sit on a higher genus surface.

1.2.2 Morse theory

Let M be an n -manifold and let $f: M \rightarrow \mathbb{R}$ be a smooth function. Recall that the critical points of f are those $x \in M$ so that $df(x) = 0$. A critical point p is *non-degenerate* if the Hessian matrix of partial derivatives $H_f(p) = \left(\frac{\partial^2 f}{\partial x_i \partial x_j}(p) \right)$ is non-singular. Equivalently, we may think of df as a section of the cotangent bundle of M , and a singular point is non-degenerate if df and the zero section intersect transversely at p . It follows immediately from either definition that non-degenerate critical points are isolated. Morse functions

are generic, in the sense that any smooth function can be approximated well by a Morse function.

For the rest of the section, suppose that f is a Morse function. Let p be a critical point of f . The *index* of f at p is the number of negative values of $H_f(p)$, counted with multiplicity. Equivalently, the index is the largest negative-definite eigenspace of the bilinear form $\langle v, w \rangle = v^t H_f(p) w$.

We are now in position to state some classical Morse-theoretic results, all from [44].

Lemma. *Suppose that $f: M \rightarrow \mathbb{R}$ is a Morse function and that p is a critical point of f with index k . There is a neighborhood of p with a coordinate system (x_1, \dots, x_n) so that p lies at 0 and f has the form*

$$f(x) = f(p) + \sum_{i=1}^k -x_i^2 + \sum_{j=k+1}^n x_j^2.$$

Write M_c for the *sub-level set* $f^{-1}(-\infty, c)$. Recall that $y \in \mathbb{R}$ is a *critical value* of f if there is critical point $x \in M$ so that $f(x) = y$.

Theorem. *Suppose that the interval $(c - \epsilon, c)$ contains no critical values. Then $M_{c-\epsilon}$ is diffeomorphic to M_c .*

Suppose instead that $(c - \epsilon, c)$ contains one critical value corresponding to a single critical point of index k . Then M_c is diffeomorphic to $M_{c-\epsilon}$ with a single k -handle attachment.

Let ψ_t be the negative gradient flow of f . Let $N_p = \{y \in Y : \lim_{t \rightarrow -\infty} \psi_t(y) = p\}$ and $T_p = \{y \in Y : \lim_{t \rightarrow \infty} \psi_t(y) = p\}$. These are called the *unstable* and *stable* manifolds of p . Loosely, the N_p is the set of points which flow down from p , and T_p is the set of points which flow down to p .

Lemma. *Let p be a critical point of index k . The dimension of N_p is k , and the dimension of T_p is $n - k$.*

Now suppose that Y is a three-manifold and that f is Morse function so that for every critical point p of index k we have $f(p) = k$. (Such a function is called *self-indexing*.) We will also assume that f has only one critical point of index 0 and index 3. Then $f^{-1}(\frac{3}{2})$ is

a Heegaard splitting of Y : the sub-level set $Y_{3/2}$ consists of a 0-handle with some 1-handles attached, so it is clearly a handlebody. Considering the function $3 - f$ we see that the interior of $Y \setminus Y_{3/2}$ is also a handlebody. We will write Σ for $f^{-1}(\frac{3}{2})$.

Let $p \in Y$ be an index 1 critical point. Then the stable manifold of p has dimension 2, and it intersects Σ in a curve. By the above theorem, this curve is exactly the attaching curve of the handle corresponding to p . Similarly, the unstable manifold of an index 2 critical point intersects Σ in a curve, the co-attaching curve of the corresponding handle. So if all three-manifolds have a self-indexing Morse function (they do) then every three-manifold has a Heegaard diagram.

1.2.3 Dehn surgery

Another important perspective on three-manifolds comes from Dehn surgery. We refer the reader to [56] and [23] for details, proofs, and clarity.

Let $K \subset Y$ be a knot and let $\nu(K)$ be a normal neighborhood of K , i.e. a solid torus with K at its core. Let $\phi: \partial\nu(K) \rightarrow \partial\nu(K)$ be an orientation-reversing homeomorphism. The manifold $Y_\phi(K) = (Y \setminus \nu(K)) \cup_\phi S^1 \times D^2$ is called the result of *Dehn surgery on Y along K* . The situation may be simplified as follows: let $[\mu], [\lambda]$ be a basis for $H_1(\partial\nu(K))$. Here μ is the meridian, which is uniquely determined by the condition that it bound a disk in $\nu(K)$. Then ϕ (and thus $Y_\phi(K)$) is determined up to isotopy by $\phi_*([\mu])$. Writing $\phi_*([\mu]) = p[\mu] + q[\lambda]$, we may thus⁶ index the results of surgery by the number $p/q \in \mathbb{Q} \cup \{\infty\}$. In S^3 , we will always take λ to be the Seifert longitude, i.e. the homology class of the intersection of a Seifert surface for K with $\partial\nu(K)$.

Among other reasons, Dehn surgery is important because of the following classical theorem of Lickorish and Wallace.

Theorem. *Every three-manifold may be obtained by surgery on a link⁷ in S^3 .*

⁶To be careful, one should also show that $\phi_*([\mu])$ is always primitive.

⁷To do surgery on a link, simply do surgery on each component.

1.3 Contact structures

The study of contact geometry began in physics. Suppose one wants to study the motion of eight planets and one minor-planet around a fixed sun. We assume that this solar system is planar, so all the planets move in two dimensions. To describe a state of the system, we need to describe the position and momentum of each planet. This takes four parameters per planet, so we will need 36 parameters in all. Equivalently, the space of possible configurations of these planets has 36 dimensions. We can think of the motion of the planets as a single path through this 36-dimensional space called the *phase space* of the system.

This is the beginning of a longer story in classical mechanics, but the point is that the evolution of a physical system can be understood as the path of a single point in a big phase space. Because we need to record both the position and momentum of each planet, this phase space will always be even-dimensional. Moreover, these dimensions are paired, e.g. the horizontal position parameter is paired with the horizontal momentum parameter. This structure, along with the barebones mathematical framework to describe classical mechanics, is called a *symplectic structure*, and the study of symplectic structures on manifolds is called *symplectic topology and geometry*. This field, abstracted away from physics, has been a great source of new tools and questions in topology.

Returning to the solar system, every freshman physics student knows that within this system there is kinetic energy related to the momenta of the planets and potential energy related to their relative positions. So there is a function which assigns a total energy to every point in the phase space. The principle of conservation of energy says that the total energy in this system will never change. Suppose the solar system starts at some point in the phase space with energy E_0 . As the system moves around the phase space, it will only ever reach other points with energy E_0 . In general, this space of such points will be 35-dimensional, one less than the size of the phase space.

The restricted phase space cannot have a symplectic structure because it has odd dimension. The analogous object is a *contact structure*. Contact structures have popped up here and there in classical physics, but did not receive much attention in mathematics

before breakthroughs by Eliashberg and Giroux.

Having said all that, in this thesis we are interested only in contact structures on three-manifolds, and we don't make any connections to physics. For more details on the mathematics, see [46].

Definition. Let Y be a three-manifold. A *contact structure* on Y is a two-plane field ξ which is totally non-integrable; i.e., for any open set $U \subset Y$, there is no surface $\Sigma \subset U$ so that $T\Sigma = \xi$.

Locally, a contact structure ξ is the kernel of a 1-form α so that $\alpha \wedge d\alpha \neq 0$. Such a 1-form is called a *contact form*. The relationship between contact structures and contact forms is somewhat delicate, but it is not important for what follows.

Two contact structures are *isotopic* if they are isotopic as plane fields via an isotopy through contact structures. Two contact structures ξ, ξ' on Y are *contactomorphic* if there is a diffeomorphism $\phi: Y \rightarrow Y$ so that $\phi_*\xi = \xi'$. By a theorem of Grey [24], these two notions of equivalence are identical.

The *standard contact structure on \mathbb{R}^3* , denoted by ξ_{std} , is the kernel of $\alpha_{std} = dz - x dy$. This structure is contactomorphic to the *cylindrical contact structure ξ_{cyl}* , the kernel of $\alpha_{cyl} = dz + r^2 d\theta$. The cylindrical structure is much easier to visualize: at the origin, $\xi_{cyl} = \ker(dz)$, the xy -plane. Moving along a ray in the xy -plane, the parameter r increases and the contact planes tilt along the ray. The angle increases towards 90° as $r \rightarrow \infty$. As α_{cyl} is invariant under vertical translation and θ -wise rotation, this suffices to describe the whole structure.

1.3.1 Transverse links

There are two natural ways in which a link can interact with a contact structure. The link may be embedded so that it is everywhere tangent to the contact planes, in which case we call the link *Legendrian*. Or the link may transversely intersect the contact planes, in which case we call the link *transverse*. We focus on the latter sort, which are in some ways more mysterious.

Two links are said to be *transversely isotopic* if they are isotopic through a family of

transverse knots. (Don't fret, there's a diagrammatic way to understand this.) This implies that transverse isotopy is a more restrictive notion than smooth isotopy. In fact, every knot has infinitely many non-transversely isotopic representatives.

Beyond smooth isotopy class, there is one [20] "classical" invariant of transverse links: the self-linking number. Suppose that the transverse link K is homologically trivial (as most of the knots in this thesis are). Let Σ be a surface bounded by K . Let v be a vector field along Σ in ξ . Then the *self-linking of T* , or $sl(T)$, is the linking number of T with a pushoff of T in the direction v . (For a diagrammatic definition, skip a few paragraphs ahead.)

There are transverse links with the same isotopy class and self-linking number ([33], [12], [18]), so the classical invariants do not totally characterize transverse links. A smooth link which supports such transverse links is called *transversely non-simple*. An invariant which can distinguish links in a transversely non-simple family is called *effective*. It is known that certain transverse invariants from Heegaard Floer homology are effective, but it is not known if the transverse invariant from Khovanov homology is effective (see Section 2.1.2).

There is a "transverse Markov theorem" relating braids and transverse links in \mathbb{R}^3 . It is easiest to visualize in the cylindrical contact structure ξ_{cyl} . Any transverse link which lies sufficiently far from the z -axis must wind around the z -axis just like a braid closure. Conversely, any braid may be transversely embedded far away from the z -axis. To close the braid, wrap strands around the z -axis. Close study of such arguments led Orevkov and Shevchishin [45] and Wrinkle [62], independently, to the following.

Theorem. *The above procedure gives a one-to-one correspondance between transverse links up to transverse isotopy and braids up to positive stabilization.*

To summarize: let β be a braid. Then any sequence of conjugations and positive stabilizations of β produce a braid whose closure is transversely isotopic to β . Moreover, any braid which closes to the same transverse link may be obtained by conjugations and positive (de)stabilizations of β .

If L is a transverse link which is the closure of the braid $\beta \in B_n$, then $sl(\beta) = \exp(\beta) - n$ where $\exp(\beta)$ is the sum of the exponents on any word equal to β . This formula shows that

a link and its negative stabilization are never transversely isotopic. The essential geometric difference between positive and negative stabilization in ξ_{cyl} is that in positive stabilization the “lasso” is always oriented along the braid axis, and therefore can cross it while still maintaining transversality with ξ_{cyl} .

Chapter 2

Some homologies

In this section, we define Khovanov homology, a homology theory for links, and Heegaard Floer homology, a homology theory for three-manifolds. These two tools have independently sparked waves of new activity in low-dimensional topology, and have connections with representation theory and contact/symplectic topology. Moreover, the two theories are connected by an algebraic gadget called a spectral sequence. This spectral sequence animates all the work in later chapters.

This is also the section in which we give up the pretense that any of this document will be readable by non-mathematicians.

2.1 Khovanov homology of links

There are many great introductions to Khovanov homology (e.g. [10]), so we will only recall enough to set some notation and to do our due diligence.

Let $L \subset S^3$ be a link with diagram \mathcal{D} . Suppose first that \mathcal{D} has no crossings. Let V be a two-dimensional vector space over¹ $\mathbb{Z}/2\mathbb{Z}$ with generators v_+ and v_- . Write $|\mathcal{D}|$ for the number of components in \mathcal{D} . The Khovanov chain complex $\text{CKh}(\mathcal{D})$ associated to \mathcal{D} is $V^{\otimes |\mathcal{D}|}$ with no differential, and the Khovanov homology of \mathcal{D} is $V^{\otimes |\mathcal{D}|}$.

Now suppose that \mathcal{D} has $c > 0$ crossings. To be precise, we should order the crossings, but the end result does not depend on the choice of order and we shall speak of it no more.

¹Khovanov homology is not much more complicated over \mathbb{Z} .

Each crossing may be *resolved* in one of two ways, called the 0- and 1-resolution, as shown in Figure 2.1. A *complete resolution* of \mathcal{D} is a choice of resolution for each crossing. For a complete resolution r , write $\mathcal{D}(r)$ for the resulting diagram. The diagram $\mathcal{D}(r)$ always has no crossings. The complete resolutions of \mathcal{D} are indexed by the *cube of resolutions* $\{0, 1\}^c$.

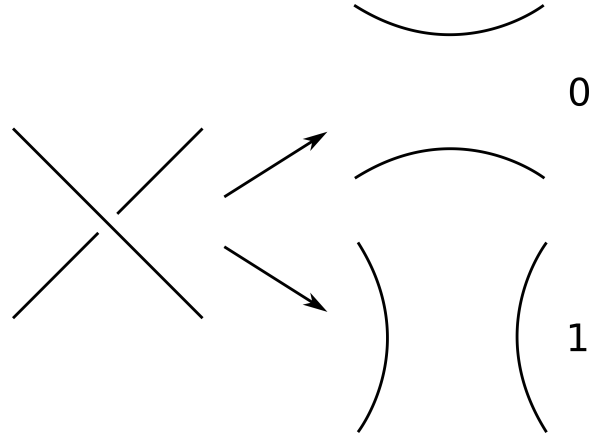


Figure 2.1: The 0- and 1-resolution of a crossing.

The vector space underlying the Khovanov chain complex is

$$\mathrm{CKh}(\mathcal{D}) = \bigoplus_{r \in \{0,1\}^c} V^{\otimes |\mathcal{D}(r)|}.$$

The simple tensors in $\mathrm{CKh}(\mathcal{D})$ are labelings of the components of a resolved diagram with v_+ and v_- . We refer to these as *canonical generators* of $\mathrm{CKh}(\mathcal{D})$.

In the classical story, $\mathrm{CKh}(\mathcal{D})$ is a bigraded complex. Orient the link, and define a crossing to be *positive* if the over-crossing strand and under-crossing strand determine the usual orientation on the page. Let $x \in V^{\otimes |\mathcal{D}(r)|}$ be a canonical generator. The first grading, called the *homological grading*, is defined by $h(x) = |r| - n_-$ where $|r|$ is the sum of the entries of r and n_- is the number of negative crossings in \mathcal{D} . The second grading is called the *internal* or *quantum grading*. First, grade V by $\tilde{q}(v_+) = 1$ and $\tilde{q}(v_-) = -1$. Now additively extend \tilde{q} to tensor products. The quantum grading of a canonical generator is defined by

$$q(x) = \tilde{q}(x) + |r| + n_+ - 2n_-$$

where n_+ is the number of positive crossings in \mathcal{D} .

We can delay no longer in defining the differential on $\text{CKh}(\mathcal{D})$. The classical proposition 1 ≥ 0 (see [14]) allows us to partially order the entire cube: for two resolutions r and r' , we have $r' \geq r$ precisely if every entry in r' is greater than or equal to every entry in r . If $r' \geq r$ and r and r' differ in only one entry, we say that r' is an (*immediate*) *successor* of r .

If r' is an immediate successor of r , then $\mathcal{D}(r)$ and $\mathcal{D}(r')$ differ at a single resolved crossing. Either $\mathcal{D}(r')$ may be obtained from $\mathcal{D}(r)$ by splitting a component into two or by merging two components into one. To define maps $d_{r,r'} : V^{|\mathcal{D}(r)|} \rightarrow V^{|\mathcal{D}(r')|}$, we focus on the tensor factors corresponding to the split or merged components. If $\mathcal{D}(r')$ is related by $\mathcal{D}(r)$ by merging two components, then $d_{r,r'}$ acts by a map m on the factors corresponding to the merged components and as the identity otherwise. If instead $\mathcal{D}(r')$ is obtained from $\mathcal{D}(r)$ by splitting a component, then $d_{r,r'}$ acts by a map Δ on the split factor and the identity otherwise. Let $m : V \otimes V \rightarrow V$ be the map defined by

$$\begin{aligned} m(v_+ \otimes v_+) &= v_+ \\ m(v_+ \otimes v_-) &= m(v_- \otimes v_+) = v_- \\ m(v_- \otimes v_-) &= v_- \end{aligned}$$

and linearity. Let $\Delta : V \rightarrow V \otimes V$ be the map defined by

$$\begin{aligned} \Delta(v_+) &= v_+ \otimes v_- + v_- \otimes v_+ \\ \Delta(v_-) &= v_- \otimes v_- \end{aligned}$$

and linearity.

Now let $d : \text{CKh}(\mathcal{D}) \rightarrow \text{CKh}(\mathcal{D})$ be the sum of all these maps, i.e.

$$d = \sum_{r \in \{0,1\}^c} \sum_{r' \text{ a successor of } r} d_{r,r'}.$$

Khovanov showed that $d \circ d = 0$, and more yet.

Theorem. [34] *Suppose that \mathcal{D} and \mathcal{D}' are two diagrams for the link L . Then there is a bigraded quasi-isomorphism between the complexes $(\text{CKh}(\mathcal{D}), \partial)$ and $(\text{CKh}(\mathcal{D}'), \partial')$.*

Khovanov proves this by assigning a bigraded quasi-isomorphism to each Reidemeister move. Later results of Jacobsson [32], Bar-Natan [11], and Khovanov [36] show that these quasi-isomorphisms are “natural” in the sense that any two sequences of Reidemeister moves from \mathcal{D} to \mathcal{D}' induce chain-homotopic quasi-isomorphisms. The homology of $(\mathrm{CKh}(\mathcal{D}), \partial)$ for any diagram \mathcal{D} of L is called the *Khovanov homology of L* and is denoted $\mathrm{Kh}(L)$.

Khovanov constructed his homology theory (in part) to better understand the famous *Jones polynomial*. The Euler characteristic of the bigraded complex $C_{i,j}$ is defined to be $\sum_{i,j} (-1)^i q^j \mathrm{rank}(C_{i,j})$. The Euler characteristic of the Khovanov homology of a link is the *unnormalized Jones polynomial*; to get the genuine object, divide by $(q + q^{-1})$.

2.1.1 Reduced Khovanov homology

There are two ways to define the *reduced Khovanov homology*. They yield bigraded quasi-isomorphic theories, but we will see in Chapter 4 that they are distinguishable in the presence of additional geometric data.

Let L be a link with diagram \mathcal{D} . Choose a basepoint p on the image of L in \mathcal{D} . For convenience, we will assume that the last tensor factor of each generator of $\mathrm{CKh}(\mathcal{D})$ corresponds to the component containing p . There is a chain map $x_p : \mathrm{CKh}(\mathcal{D}) \rightarrow \mathrm{CKh}(\mathcal{D})$ defined on generators by

$$\begin{aligned} x_p(y \otimes v_+) &= y \otimes v_- \\ x_p(y \otimes v_-) &= 0 \end{aligned}$$

The *reduced subcomplex* $\widetilde{\mathrm{CKh}}_p(\mathcal{D})$ is $\ker(x_p)$. The *reduced quotient complex* $\underline{\mathrm{CKh}}_p(\mathcal{D})$ is $\mathrm{coker}(x_p)$. The homologies of these complexes are both called reduced Khovanov homology; the ambiguity is justified by the fact that their homologies are isomorphic as h - and q -graded complexes (with a constant shift in the q -gradings) [35]. It is clear that $\widetilde{\mathrm{CKh}}_p(\mathcal{D})$ has a basis of canonical generators. The projections of canonical generators of the form $y \otimes v_+$ form a basis of $\underline{\mathrm{CKh}}_p(\mathcal{D})$. Whenever we take a representative of an element in the quotient complex, we will assume it is a sum of these canonical generators.

The reduced theories may be defined more geometrically as follows: place a little circle

on \mathcal{D} near p . The map x_p is the map given by the cobordism which merges this circle, with a v_- -label, to whichever component contains p . This is the original perspective taken by Khovanov, and it fits naturally into Bar-Natan's cobordism framework.

For knots, the reduced theory does not depend on a choice of basepoint.

2.1.2 Khovanov homology and transverse links

The first application of Khovanov's theory to transverse links comes from Plamenevskaya [52]. For the rest of this section, all links are assumed to live in S^3 .

Recall (Section 1.3.1) that there is a one-to-one correspondence between transverse links and braids up to positive stabilization and conjugation; the point is that a braid closure diagram is naturally the diagram of a transverse link. A braid closure diagram has a unique resolution in which each positive crossing is given the 0-resolution and each negative resolution is given the 1-resolution. This is called the *braidlike resolution*.

Let L be a transverse link, β a braid so that $\hat{\beta} = L$, and \mathcal{D} a braid closure diagram of β . Let r be the braidlike resolution of \mathcal{D} . Define $\psi(L)$ to be the element of $\text{CKh}(\mathcal{D}(r))$ which has all v_- labels. This element is called the *transverse invariant in Khovanov homology* on account of the following proposition.

Proposition. [52] *Let \mathcal{D} and \mathcal{D}' be braid closure diagrams which are related by a sequence of conjugations and positive stabilizations. The induced map ρ on Khovanov homology satisfies $\rho(\psi(\mathcal{D})) = \psi(\mathcal{D}')$. Moreover, $q(\psi(L)) = sl(L)$ and $h(L) = 0$.*

If L is a negative stabilization of another link, then $[\psi(L)] = 0$. If L is σ_i -negative for any i , then $[\psi(L)] = 0$. If L can be represented by a right-veering braid, then $[\psi(L)] \neq 0$. If L can be represented by a quasipositive² braid, then $[\psi(L)] \neq 0$.

It is not known if ψ is effective.

2.1.3 Khovanov homology and cobordisms

The Khovanov differential is defined by assigning linear-algebraic maps to diagrammatic merges and splits. The diagrammatic moves may be understood more geometrically as

²A braid is *quasipositive* if it can be written as a product of conjugations of positive generators.

simple cobordisms, as in Figure 2.2. Morse theory shows that any surface may be understood as a stack of merge, split, cup, cap, and identity cobordisms; in fact, this is a handle decomposition. Suppose that Σ is a cobordism between the links L_1 and L_2 , and fix a handle decomposition of Σ . Each of the simple cobordisms in the decomposition is assigned a map, and the map ϕ_Σ is composition of these maps. The references to Jacobsson, Bar-Natan, and Khovanov above show (independently) that these maps do not depend on the handle decomposition of Σ .



Figure 2.2: From left to right: merge, split, cup, cap, and identity morphisms.

This is an essential feature of Khovanov homology. In Bar-Natan's wonderful reformulation [11], he realizes Khovanov homology as a theory firstly about tangles and cobordisms and secondly about vector spaces and maps.

2.2 Heegaard Floer homology of three-manifolds

Heegaard Floer homology is an adaptation (or specialization) of Lagrangian Floer homology to study three- and four-manifolds. It fits into a larger project of computing and understanding Seiberg-Witten invariants, but it is still difficult to do many concrete computations using the original definition. The grid diagram approach has made Heegaard Floer homology easier to work with, but is a book length project on its own. To paraphrase Jacob Rasmussen, Heegaard Floer homology is similar to ordinary homology in that it offers a unifying perspective on many otherwise disparate phenomena in three-manifold topology.³

So here's the standard disclaimer: the entire theory is really complicated, and we will stick to describing the parts of the theory which we need for later chapters.

³More hype: Heegaard Floer homology is closely related to instanton Floer homology, monopole Floer homology, embedded contact homology, Khovanov homology...

2.2.1 Formal properties

Following Rasmussen’s approach in [53], we first describe some “formal” properties of Heegaard Floer homology without proof. See [47] for details.

Let Y be a closed orientable three-manifold. Heegaard Floer homology assigns to Y a graded⁴ vector space⁵ $\widehat{HF}(Y)$. It also has a direct sum decomposition

$$\widehat{HF}(Y) = \bigoplus_{\mathfrak{s} \in \text{Spin}^c(Y)} \widehat{HF}(Y, \mathfrak{s})$$

where $\text{Spin}^c(Y)$ is the set of Spin^c -structures on Y . ($\text{Spin}^c(Y)$ is a “ $H^1(Y)$ -torsor” – $H^1(Y)$ acts freely and transitively.)

Heegaard Floer homology has a Künneth formula for connected sums: $\widehat{HF}(Y \# Y') = \widehat{HF}(Y) \otimes \widehat{HF}(Y')$. (What does this say about $\widehat{HF}(S^3)$?)

Heegaard Floer homology has a functorial structure. Let W be a cobordism from Y to Y' . Then W induces a map $\widehat{F}_W : \widehat{HF}(Y) \rightarrow \widehat{HF}(Y')$. Now suppose that W' is a cobordism from Y' to Y'' . Then $W' \circ W$ is a cobordism from Y to Y'' , and $\widehat{F}_{W'} \circ \widehat{F}_W = \widehat{F}_{W' \circ W}$. An integrally-framed surgery on a knot in a three-manifold may be understood as a cobordism between the original and surgered manifolds [23], so Heegaard Floer homology assigns maps to surgeries. For certain geometrically related surgeries, these maps fit into exact triangles, see e.g. [47].

The empty manifold \emptyset has Heegaard Floer homology $\mathbb{Z}/2\mathbb{Z}$, and a closed four-manifold may be understood as a cobordism from \emptyset to \emptyset . The induced map $\mathbb{Z}/2\mathbb{Z} \rightarrow \mathbb{Z}/2\mathbb{Z}$ is not very interesting (e.g. it is totally determined by the ordinary homology) but this is the idea behind the (very interesting) Heegaard Floer four-manifold invariant.

The vector space $\widehat{HF}(Y)$ is the homology of the Heegaard Floer chain complex $\widehat{CF}(Y)$. Actually, the chain complex is constructed from a Heegaard diagram, so $\widehat{CF}(Y)$ is a significant abuse of notation: two different Heegaard diagrams may yield different chain complexes. But the homology $\widehat{HF}(Y)$ does not depend on choice of Heegaard diagram as long as all involved diagrams satisfy certain technical conditions.

⁴There is always a relative $\mathbb{Z}/2\mathbb{Z}$ grading, but this can be improved to $\mathbb{Z}/n\mathbb{Z}$, \mathbb{Z} , or \mathbb{Q} under various topological conditions. Sometimes these can be upgraded to absolute gradings.

⁵Again, we work over $\mathbb{Z}/2\mathbb{Z}$ rather than \mathbb{Z} for simplicity.

There are two computations of Heegaard Floer homology which are important for our work which we delay until we provide a proper definition.

2.2.2 Definition

Let Y be a three-manifold. Let $(\Sigma, \boldsymbol{\alpha}, \boldsymbol{\beta})$ be a genus g Heegaard diagram for Y . Let $z \in \Sigma \setminus (\boldsymbol{\alpha} \cup \boldsymbol{\beta})$. The data $(\Sigma, \boldsymbol{\alpha}, \boldsymbol{\beta}, z)$ is called a *pointed Heegaard diagram*. The Heegaard Floer chain complex $\widehat{CF}(\Sigma, \boldsymbol{\alpha}, \boldsymbol{\beta}, z)$ is generated by g -tuples (x_1, \dots, x_g) of intersection points between $\boldsymbol{\alpha}$ and $\boldsymbol{\beta}$ which satisfy the condition that if $x_i \in \alpha_j \cap \beta_k$, then no other x_i can lie in α_j or β_k . (“You may use each curve once and only once in each generator.”)

This generating set may be described geometrically. Let $\text{Sym}^g(\Sigma)$ be the g -fold symmetric power of Σ , i.e. $\text{Sym}^g(\Sigma) = \Sigma^{\times g}/S_g$ where the symmetric group S_g acts by permuting coordinates. Let $T_{\boldsymbol{\alpha}}$ be the image of $\alpha_1 \times \dots \times \alpha_g$ in $\text{Sym}^g(\Sigma)$, and define $T_{\boldsymbol{\beta}}$ similarly. Then $\widehat{CF}(\Sigma, \boldsymbol{\alpha}, \boldsymbol{\beta}, z)$ is generated by the collection of points $T_{\boldsymbol{\alpha}} \cap T_{\boldsymbol{\beta}}$.

As Σ is a surface, it can be equipped with a complex structure j . It is not hard to extend this to $\Sigma^{\times n}$, and then to $\text{Sym}^g(\Sigma)$, at least away from the diagonal. Ozsváth and Szabó show that j may be extended to an almost complex structure⁶ J on $\text{Sym}^g(\Sigma)$. A *pseudoholomorphic disk* is a map $\phi: D^2 \rightarrow \text{Sym}^g(\Sigma)$ so that $\phi \circ i = J \circ \phi$, where i is the usual complex structure on D^2 as a subset of \mathbb{C} . Pseudoholomorphic disks were first used by Gromov to great effect in symplectic topology [27].

Let $x, y \in T_{\boldsymbol{\alpha}} \cap T_{\boldsymbol{\beta}}$. Write $\partial^+ D^2$ for the boundary component of D^2 with positive real part and $\partial^- D^2$ for the boundary component of D^2 with negative real part. A continuous map $\phi: D^2 \rightarrow \text{Sym}^g(\Sigma)$ is called a *Whitney disk from x to y* if $\phi(-i) = x$, $\phi(i) = y$, $\phi(\partial^+ D^2) \subset T_{\boldsymbol{\alpha}}$, and $\phi(\partial^- D^2) \subset T_{\boldsymbol{\beta}}$. Write $\pi_2(x, y)$ for the set of Whitney disks from x to y , considered up to homotopy rel boundary.

For $\phi \in \pi_2(x, y)$, write $\widehat{\mathcal{M}}(\phi)$ for the moduli space of pseudoholomorphic disks homotopic to ϕ . The dimension of this space is controlled by the *Maslov index* $\mu(\phi)$, a gadget from symplectic topology. In favorable circumstances, the Maslov index is precisely the dimension

⁶At its heart, the definition of Heegaard Floer homology ‘should’ be “the Lagrangian Floer homology of $T_{\boldsymbol{\alpha}}$ and $T_{\boldsymbol{\eta}}$ in $\text{Sym}^g(\Sigma)$.” The Lagrangian Floer construction depends on the existence of an almost complex structure with particular properties. Ozsváth and Szabó get around this by considering *families* of almost complex structures. Yakili later showed the existence of the right complex structure.

of the moduli space. In any positive dimension, the moduli space has an \mathbb{R} -action given by the vertical translation within $D^2 \subset \mathbb{C}$. Write $\mathcal{M}(\phi) = \widehat{\mathcal{M}}(\phi)/\mathbb{R}$. Note that $\dim(\mathcal{M}(\phi)) = \dim(\widehat{\mathcal{M}}(\phi)) - 1$ as long as $\dim(\widehat{\mathcal{M}}(\phi))$ was positive to begin with.

Now let $x \in T_\alpha \cap T_\beta$. Define the differential $\partial: \widehat{CF}(\Sigma, \alpha, \beta, z) \rightarrow \widehat{CF}(\Sigma, \alpha, \beta, z)$ as follows:

$$\partial x = \sum_{y \in T_\alpha \cap T_\beta} \sum_{\substack{\phi \in \pi_2(x, y) \\ \mu(\phi)=1 \\ n_z(\phi)=0}} |\mathcal{M}(\phi)| y.$$

Here $n_z(\phi)$ is the intersection number between ϕ and the subvariety $\{z\} \times \text{Sym}^{g-1}(\Sigma) \subset \text{Sym}^g(\Sigma)$. Using various techniques from the world of Lagrangian Floer homology, one can show that $\partial^2 = 0$. Write $\widehat{HF}(\Sigma, \alpha, \beta, z)$ for the homology of $\widehat{CF}(\Sigma, \alpha, \beta, z)$.

Theorem. *Suppose that $(\Sigma, \alpha, \beta, z)$ and $(\Sigma', \alpha', \beta', z')$ are pointed Heegaard for the three-manifold Y . Suppose in addition that each diagram is weakly admissible, as defined in the next section. Then $\widehat{HF}(\Sigma, \alpha, \beta, z) \cong \widehat{HF}(\Sigma', \alpha', \beta', z')$.*

We define the Heegaard Floer homology of Y , denoted by $\widehat{HF}(Y)$, to be the Heegaard Floer homology of any weakly admissible Heegaard diagram for Y .

2.2.3 Computing Heegaard Floer homology

As detailed in [48], a holomorphic disk may be understood through a projection to Σ which we call its *domain*. The curves in α and β split Σ into regions. A domain is a sum (over \mathbb{Z}) of regions on Σ . Let $\{R_i\}$ be the regions of (Σ, α, β) and let $x_i \in R_i$. To a disk ϕ we assign the domain $\sum_i n_{x_i}(\phi) R_i$. The resulting domain does not depend on the choice of x_i .

A *periodic domain* is a domain whose boundary is a union of entire α and β curves. The set of periodic domains for a particular diagram form a group. In [48] this group is shown to be isomorphic to $H_1(Y)$. A Heegaard diagram is called *weakly admissible* if every periodic domain has both positive and negative coefficients. For the rest of this section, we will work only with admissible diagrams.

As one might expect, domains of pseudoholomorphic disks are heavily constrained.

Lemma. [48] *Let ϕ be a pseudoholomorphic disk connecting x and y . Let R be the domain of ϕ .*

- *All the coefficients of R are positive.*
- *If ϕ' is another disk connecting x and y with domain R' , then $R = R'$ if and only if ϕ and ϕ' are homotopic.*
- *Let $\partial_\alpha\phi$ be the part of the boundary of the domain of ϕ which lies along α curves (as a 1-chain). Define $\partial_\beta\phi$ identically. Let ∂ be the usual boundary operator. (Sorry.) Then $\partial\partial_\alpha\phi = -\partial\partial_\beta\phi = y - x$. Roughly, the boundary of R traces a path from x to y (along α curves) and back (along β curves).*
- *Suppose that ϕ and ϕ' are both pseudoholomorphic disks connecting x and y . Then the difference of their domains is a periodic domain. (To be fancier, the space of domains representing pseudoholomorphic disks between x and y is an affine space over the group of periodic domains.)*

These conditions do not guarantee the existence of pseudoholomorphic disks. Our main tool toward that end is the Riemann mapping theorem.

For us, the most important fact about the Maslov index $\mu(\phi)$ is the formula due to Lipshitz [40]. We need to define a few terms. Let R be the domain of a pseudoholomorphic disk in $\pi_2(x, y)$. Any $a \in x$ is an intersection point between an α and β curve, and so locally there are four regions adjacent to a . Let $n_a(R)$ be the average of the coefficients of R in these regions. Let $n_x(R) = \sum_{a \in x} n_a(R)$.

Let $S \subset \Sigma$ be an embedded subsurface with boundary along $\alpha \cup \eta$. Using the local picture of intersection points, the corners of S may be classified as *acute* and *obtuse*: an acute corner occupies only one of the four regions adjacent to the corner. Define the *Euler measure* $e(S) = \chi(S) - \frac{\text{acute}(S)}{4} + \frac{\text{obtuse}(S)}{4}$. The Euler measure is additive, so it may be extended to arbitrary regions.

Lemma ([41]). *Let D be the domain of a pseudoholomorphic disk in $\pi_2(x, y)$. Then*

$$\mu(D) = n_x(D) + n_y(D) + e(D).$$

2.2.4 Two computations

Example 1. The Künneth formula for Heegaard Floer homology implies that $\widehat{HF}(S^3) = \mathbb{Z}/2\mathbb{Z}$, but we can compute this directly from a Heegaard diagram.

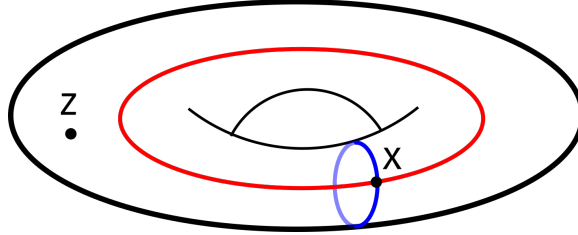


Figure 2.3

From this diagram, $\widehat{CF}(\Sigma, \alpha, \eta, z)$ is generated by the lone intersection point, x . This diagram has only one embedded region, and it contains the basepoint z . This implies that there are no periodic domains on the diagram – and there shouldn't be, as $H^1(S^3)$ vanishes – so it is vacuously weakly admissible. Moreover, the differential ∂ must be zero, and $\widehat{HF}(\Sigma, \alpha, \eta)$ is also generated by x .

Example 2. Here is a Heegaard diagram for $S^1 \times S^2$.

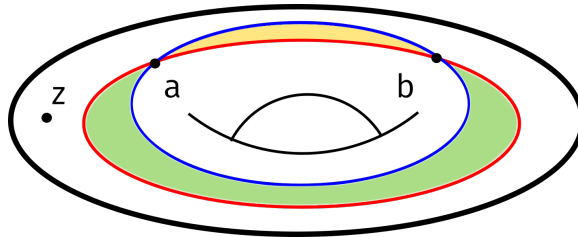


Figure 2.4

$\widehat{CF}(\Sigma, \alpha, \eta, z)$ is generated by a and b . The group of periodic domains is generated by the green region minus the yellow region. This periodic domain has positive and negative coefficients and generates the whole group (which must have the same rank as $H^1(S^1 \times S^2)$). Therefore the diagram is weakly admissible.

To compute ∂ , we must analyze maps from the disk into $\text{Sym}^1(T^2) = T^2$. The Riemann Mapping Theorem implies that there is an \mathbb{R} 's worth of such maps whose image is the green region and another \mathbb{R} 's worth whose image is the yellow region. (To show carefully that there are no other disks, study their putative image in the universal cover.) It is not hard

to show that the Maslov index of these disks is 1.

Diagrams for $S^1 \times S^2$ (or connected sums of $S^1 \times S^2$ s) which consist only of parallel curves are called *standard*. They will be important in Chapter 3

2.2.5 Heegaard Floer homology and contact structures

Let (Y, ξ) be a contact three-manifold. Ozsváth and Szabó identify an element $c(Y, \xi) \in \widehat{HF}(Y)$ (or $c(\xi)$ when Y is clear from context) which carries information about ξ [49]. The essential property of $c(\xi)$ is that it vanishes whenever ξ is *overtwisted*. Overtwistedness is an important property in contact topology, and a non-overtwisted contact structure is called *tight*.

2.3 The spectral sequence from $\widetilde{Kh}(L)$ to $\widehat{HF}(S^3(L))$

2.3.1 Why tho

It's not hard to make the case that a spectral sequence like Ozsváth and Szabó's ought to exist. Let $L \subset S^3$ be a link and let $S^3(L)$ denote the branched double cover of L . The evidence:

- For a flat diagram \mathcal{D}' with k components, $\widetilde{Kh}(\mathcal{D}') \cong (\mathbb{Z}/2\mathbb{Z} \oplus \mathbb{Z}/2\mathbb{Z})^{\otimes k-1}$.
- The branched double cover of \mathcal{D}' is $\#^{k-1}(S^1 \times S^2)$, which has Heegaard Floer homology $(\mathbb{Z}/2\mathbb{Z} \oplus \mathbb{Z}/2\mathbb{Z})^{\otimes k-1}$. The relative gradings of the Floer and Khovanov homologies are essentially the same.
- The Khovanov differential is constructed from cobordism between link diagrams. These lift to surgery cobordisms between branched double covers. Heegaard Floer homology assigns maps to these cobordisms. So we can “take the branched cover” of the entire Khovanov chain complex setup and get a Heegaard Floer setup.
- Heegaard Floer cobordism maps between $\#(S^1 \times S^2)$ s are determined by simple topological data.

Hopefully this convinces you that Khovanov homology can be computed in a Floer context. The much more remarkable part is that this same cube of resolutions can be used to compute

$\widehat{\text{HF}}(S^3(L))$. For a diagram with only one crossing, this is equivalent to a well-known surgery exact sequence in Heegaard Floer homology. For a diagram with many crossings, one collates these exact sequences into a spectral sequence. This is possible because Heegaard Floer homology can assign maps to more complicated cobordisms, and these maps satisfy certain interpolation conditions called A_∞ -relations.

2.3.2 Branched double covers and surgery

We now demonstrate the connection between change of resolution on a diagram and Dehn surgery along an auxiliary knot. Let L be a link in S^3 . The branched double cover $S^3(L)$ may be constructed as follows: take two disjoint copies of S^3 . Let S be a Seifert surface for L . This surface is orientable, and we are justified in talking about its top and bottom. Now implement the following teleportation regime: if a spaceship flies into the top of one copy of S , it comes out the bottom of the other copy, and vice versa. See Figure 2.5.

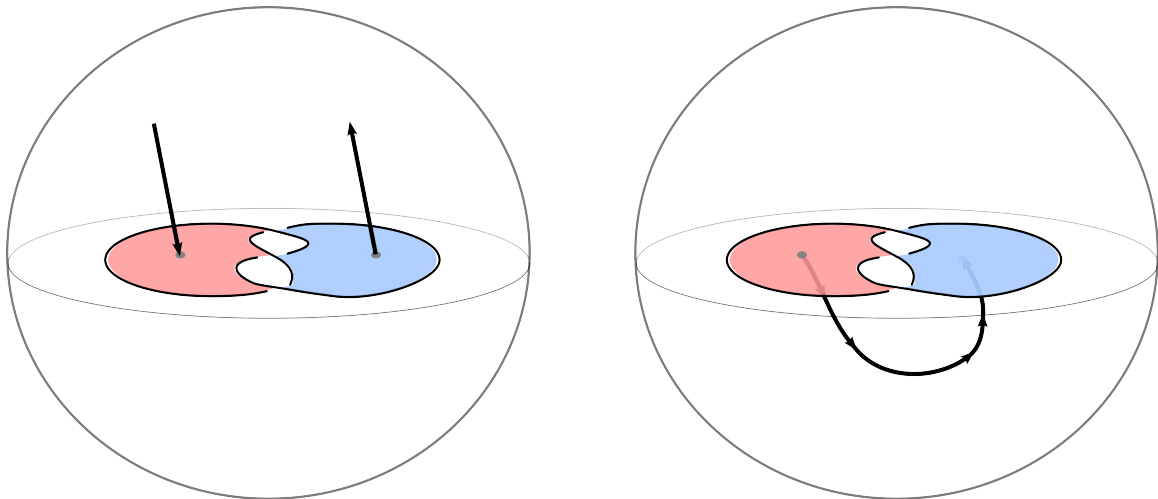


Figure 2.5: A schematic for the branched cover of S^3 over a trefoil knot.

A similar picture shows that $S^3(\mathcal{U}) \cong S^3$. For the m -component unlink \mathcal{U}^m we have $S^3(\mathcal{U}^m) = \#^{m-1} S^1 \times S^2$.

Now suppose that r' is a successor of r so that $\mathcal{D}(r)$ and $\mathcal{D}(r')$ differ only by a merge or split operation. These may be realized as two-dimensional surgery along an auxiliary arc, see 2.6. In the branched double cover, this arc lifts to a knot and the two-dimensional surgery lifts to 0-framed Dehn surgery.

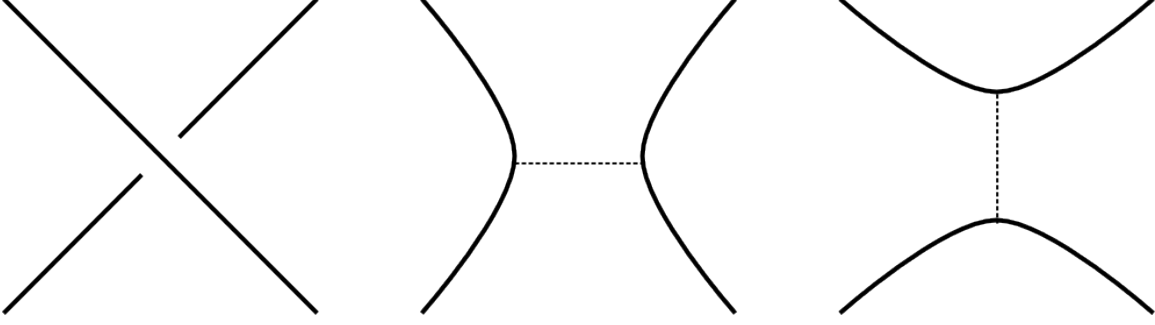


Figure 2.6: A crossing and its two resolutions. One may realize the change of resolution from middle to right by a two-dimensional surgery along the dotted arc. Its image in the resulting diagram is also shown.

2.3.3 Pseudoholomorphic polygons

Let Σ be a closed surface and suppose that η_1, \dots, η_n are sets of curves so that for any i the diagram $(\Sigma, \eta_i, \eta_{i+1})$ is a weakly admissible Heegaard diagram. Let $z \in \Sigma \setminus (\bigcup_i \eta_i)$ be a basepoint. Ozsváth and Szabó define a map

$$f_{n-2}: \widehat{CF}(\Sigma, \eta_1, \eta_2, z) \otimes \widehat{CF}(\Sigma, \eta_2, \eta_3, z) \otimes \cdots \otimes \widehat{CF}(\Sigma, \eta_{n-1}, \eta_n, z) \rightarrow \widehat{CF}(\Sigma, \eta_1, \eta_n, z)$$

by

$$f_{n-2}(x_1 \otimes \cdots \otimes x_n) = \sum_{y \in T_{\eta_1} \cap T_{\eta_n}} \sum_{\substack{\phi \in \pi_2(x_1, \dots, x_n, y) \\ n_z(\phi) = 0 \\ \mu(\phi) = 0}} |\mathcal{M}(\phi)| y.$$

Here $\pi_2(x_1, \dots, x_n, y)$ is the space of *Whitney* $(n+1)$ -gons with corners at x_1, \dots, x_n and y . The moduli space $\mathcal{M}(\phi)$ is hatless because spaces of Whitney polygons do not admit a \mathbb{R} -action. We will still identify f_0 with the differential $\partial: \widehat{CF}(\Sigma, \eta_1, \eta_2, z) \rightarrow \widehat{CF}(\Sigma, \eta_1, \eta_2, z)$. Just as in the bigon case, every polygon ϕ has a domain on Σ , and for sufficiently nice diagrams the space $\mathcal{M}(\phi)$ is finite as long as $\mu(\phi) = 0$.

The Maslov index may be computed by Sarkar's formula [58]. Let D be the domain of a pseudoholomorphic polygon connecting connecting the points $x_{1,2}, x_{2,3}, \dots, x_{n,1}$ where $x_{i,i+1}$ is a collection of intersection points between curves in η_i and η_{i+1} . Define $n_{x_{i,i+1}}$ just as n_x in Lipshitz's formula. Orient the edges of D and let ∂_i be the boundary of D along curves in η_i .

Lemma ([58]). *Let D be the domain of a pseudoholomorphic polygon in $\pi_2(x_{1,2}, x_{2,3}, \dots, x_{n,1})$. Let k be the number of curves in each collection $\boldsymbol{\eta}_i$. Then*

$$\mu(D) = n_{x_{1,2}}(D) + n_{x_{n,1}}(D) - e(D) + \sum_{n \geq j > \ell > 1} \partial_j(D) \cdot \partial_\ell(D),$$

where \cdot denotes the algebraic intersection number and $e(D)$ is again the Euler measure.

These maps satisfy the A_∞ relations:

$$\sum_{j=0}^{n-1} \sum_{i=0}^{n-1} f_{n-i+1}(x_1, \dots, x_j, f_i(x_{j+1}, \dots, x_{j+i}), x_{j+i+1}, \dots, x_n) = 0.$$

The left-hand side of the equation is the sum of all the ways to combine (or Associate) a pair of f s to combine n elements into one. For $n = 1$ this simplifies to $f_0 \circ f_0 = 0$, or just the statement that f_0 is a differential. For $n = 2$ we get

$$f_0(f_1(x_1, x_2)) = f_1(f_0(x_1), x_2) + f_1(x_1, f_0(x_2))$$

or equivalently that f_1 is a chain map on the complex $\widehat{CF}(\boldsymbol{\eta}_1, \boldsymbol{\eta}_2) \otimes \widehat{CF}(\boldsymbol{\eta}_2, \boldsymbol{\eta}_3)$. The next relation shows that f_1 is “associative” up to homotopy.

2.3.4 Bouquet diagrams

The A_∞ structure described above is quite intricate. To get handle on it, Ozsváth and Szabó use special Heegaard diagrams for branched double covers. We describe these diagrams in the most general case, but the reader won’t miss much by replacing all instances of Y with S^3 .

Let $K \subset Y$ be a link with k components. Choose some basepoint $w \in Y \setminus K$. Connect each component of K to w through pairwise disjoint arcs. The union of K with such a collection of arcs is called a *bouquet* for K .

Definition. Let Γ be a bouquet for K . A pointed Heegaard diagram $(\Sigma, \{\alpha_i\}_{i=1}^n, \{\eta_i\}_{i=1}^n, z)$ presenting Y is *subordinate to the bouquet* Γ if it satisfies the following conditions.

- The diagram $(\Sigma, \boldsymbol{\alpha}, \{\eta_i\}_{i=k+1}^n, z)$ presents $Y \setminus \nu(\Gamma)$.

- Surger out the curves $\{\eta_i\}_{i=k+1}^n$ from Σ . Each remaining η_i lies on a punctured torus $\partial N_i \subset N(\Gamma)$ which surrounds the component K_i for $1 \leq i \leq k$.
- For $1 \leq i \leq k$, the curve η_i is a meridian of the component K_i .

Loosely, the first k of the η curves describe a normal neighborhood of Γ and the remaining η curves fill out the rest of Y . Such a diagram exists for every pair (Y, K) , and the resulting spectral sequence does not depend on a choice of bouquet [51]. We refer to such diagrams as *K-bouquet* diagrams for short.

Suppose that the curves $\{\eta_i\}_{i=1}^k$ in a K -bouquet diagram are ∞ -framed curves along the tori N_i . Let γ_i be a longitude on N_i let $\delta_i = \eta_i + \gamma_i$, so that $|\eta_i \cap \delta_i| = |\delta_i \cap \gamma_i| = |\gamma_i \cap \eta_i| = -1$ and that each of these curves is disjoint from z . For $I \in \{0, 1, \infty\}^k$, define the set of curves $\eta(I)$ by

$$\eta_j(I) = \begin{cases} \eta_i & \text{if } i > k \text{ or } I_j = \infty \\ \gamma_i & \text{if } I_j = 0 \\ \delta_i & \text{if } I_j = 1 \end{cases}$$

The diagram $(\Sigma, \alpha, \eta(I), z)$ is a pointed Heegaard diagram for the result of I -framed surgery along K .

Now let \mathcal{D} be a diagram for a link $L \subset S^3$ with c crossings. We have already seen that a change in resolution of \mathcal{D} may be realized by surgery along an auxiliary knot. If we make several changes, they may be realized together by surgery along a link. Define a *path of resolutions* \mathbf{I} to be a chain of successors, i.e. $\mathbf{I} = \{I_1, I_2, \dots, I_n : I_{i+1} \text{ is a successor of } I_i\}$. To simplify notation, we allow for paths of length one. From a path of resolutions $\mathbf{I} = \{I_1, \dots, I_n\}$ one can build the *bouquet multidiagram*

$$(\Sigma, \alpha, \eta(I_1), \eta(I_2), \dots, \eta(I_n), z).$$

In general, $\eta(I_j)$ and $\eta(I_{j+1})$ will have curves in common, which is unsuitable for Floer homology. We implicitly perturb identical curves so that they intersect twice pairwise and so that the resulting multidiagram is admissible. We will say that two such curves are *parallel*. Roberts showed that these perturbations can be done in a systematic way [54].

Because $\eta(I_i)$ and $\eta(I_{i+1})$ consist of almost identical curves, the group

$$\widehat{CF}(\eta(I_i), \eta(I_{i+1})) = \widehat{CF}(\#^{k-1}S^2 \times S^1)$$

has a generator (and cycle) of highest degree which we denote by Θ_i , see our model calculation in Section 2.2.4 and [47]. For each path \mathbf{I} of length greater than one there is a map $d_{\mathbf{I}} : \widehat{CF}(\alpha, \eta(I^1)) \rightarrow \widehat{CF}(\alpha, \eta(I^n))$ defined by

$$d_{\mathbf{I}}(x) = f_{\mathbf{I}}(x \otimes \Theta_1 \otimes \cdots \otimes \Theta_{n-1}).$$

For paths of length 1, define ∂_I to be the usual differential on \widehat{CF} . For two resolutions I, I' (possibly equal), write $\mathcal{P}(I, I')$ for the set of paths from I to I' and define

$$\partial_{I, I'} = \sum_{\mathbf{I} \in \mathcal{P}(I, I')} \partial_{\mathbf{I}}.$$

Write $X = \bigoplus_{I \in \{0,1\}^k} \widehat{CF}(\Sigma, \alpha, \eta(I), z)$ and define $D : X \rightarrow X$ by $D = \sum \partial_{I, I'}$. Using the structure of bouquet diagrams and multidagrams, Ozsváth and Szabó show that (X, D) is a complex and that $H_*(X', D') \cong \widehat{HF}(S^3(L))$. Here are the essential steps:

1. The coefficient of y in $D^2(x)$ is the number of *broken polygons* connecting x and y in which the degenerating chord intersects α . By broken polygon we mean two polygons joined at a vertex. To show that $D \circ D = 0$, it suffices to show that the sum of these particular degenerations is zero.
2. The space of pseudoholomorphic polygons may be compactified by adding a boundary. The boundary is a space of broken polygons which includes those counted in the previous step. Broken polygons are degenerations of larger polygons along a chord, see Figure 3.7. Because they form the boundary of a compact space, the sum of all these degenerations must vanish.
3. The other degenerations are those for which the degenerating chord spans η curves. Ozsváth and Szabó show the following, using the particular structure of bouquet diagrams:

Lemma (Cancellation lemma). ⁷ Let I and J be resolutions of \mathcal{D} . Then

$$\sum_{(I_0, \dots, I_k) \in \mathcal{P}(I, J)} f_{\mathbf{I}}(\Theta_0 \otimes \Theta_1 \otimes \cdots \otimes \Theta_n) = 0,$$

where $\Theta_i \in \widehat{HF}(\boldsymbol{\eta}_i, \boldsymbol{\eta}_{i+1})$ is a canonical generator.

The cancellation lemma shows that all degenerations whose chord spans $\boldsymbol{\eta}$ curves sum to zero. This leaves only the degenerations along chords which intersect $\boldsymbol{\alpha}$, which must therefore sum to zero. Therefore $D \circ D = 0$.

4. Suppose the link L has only one component.

Theorem. Let L be a framed knot in a three-manifold Y , and let

$$\hat{f}: \widehat{CF}(Y_0(L)) \rightarrow \widehat{CF}(Y_1(L))$$

denote the chain map induced by the surgery cobordism. Then $\widehat{CF}(Y)$ is quasi-isomorphic to the mapping cone of \hat{f} .

This is a stronger version of the surgery exact sequence [47]. For $Y = S^3$, this shows that $H_*(X, D) \cong \widehat{HF}(S^3(K))$ when K has a single crossing.

5. Use induction on the number of components of L :

Suppose that L has ℓ components. Let

$$X(\{0, 1, \infty\}^\ell) = \bigoplus_{I \in \{0, 1, \infty\}^\ell} \widehat{CF}(\Sigma, \boldsymbol{\alpha}, \boldsymbol{\eta}(I), z)$$

and for any subset $S \subset \{0, 1, \infty\}^\ell$ write

$$X(S) = \bigoplus_{I \in S} \widehat{CF}(\Sigma, \boldsymbol{\alpha}, \boldsymbol{\eta}(I), z).$$

We abuse notation by writing $D: X(\{0, 1, \infty\}^\ell) \rightarrow X(\{0, 1, \infty\}^\ell)$ for the map analogous to $D: X \rightarrow X$ for the ‘cube’ $\{0, 1, \infty\}^\ell$. The mapping cone lemma above shows

⁷This is one of at least three lemmas in *this field* which are called “the cancellation lemma.”

that $H(X(\{0, 1, \infty\}^\ell), D') = 0$ for $\ell = 1$. Now assume the lemma for $k = \ell$. As

$$X(\{0, 1\}^\ell \times \{0, 1\infty\})/X(\{0, 1\}^{\ell+1}) \cong X(\{0, 1\}^\ell \times \{\infty\}),$$

there is a short exact sequence of complexes

$$0 \rightarrow X(\{0, 1\}^{\ell+1}) \rightarrow X(\{0, 1\}^\ell \times \{0, 1\infty\}) \rightarrow X(\{0, 1\}^\ell \times \{\infty\}) \rightarrow 0.$$

It follows from arguments similar to the strengthening of the surgery exact sequence that $H(X(\{0, 1\}^\ell \times \{0, 1\infty\})) = 0$, so $X(\{0, 1\}^{\ell+1}) \cong X(\{0, 1\}^\ell \times \{\infty\})$.

The complex (X, D) is filtered by the partial ordering on $\{0, 1\}^k$ and so its homology can be computed via a spectral sequence. This is the Ozsváth-Szabó spectral sequence which we denote by E .

Theorem. *Let E be the spectral sequence induced by the order filtration on X .*

- $E^0 = X$ as a group. The differential d_0 is the sum of the internal differentials on each Heegaard Floer chain group. Each of these groups is equal to $\widehat{CF}(\#^m(S^2 \times S^1))$ for some $m \geq 0$.
- $E^1 \cong \widehat{CKh}(m(L))$, the reduced Khovanov chain group of the mirror of L .
- $E^2 \cong \widehat{Kh}(m(L))$, the reduced Khovanov homology of the mirror of L .
- $E^\infty \cong \widehat{HF}(S^3(L))$, the Heegaard Floer homology of the branched double cover of L .

In any spectral sequence arising from such a filtration, the differential on the zeroth page of this spectral sequence is the part of D which preserves the order filtration. This explains the first two facts. To prove the third, one must analyze the Heegaard Floer maps which count holomorphic triangles. In fact, the cobordism maps between connected sums of $S^1 \times S^2$ s are determined by data in ordinary homology, which ultimately implies that they “agree” with the maps on Khovanov homology.

For details of some of these constructions, see Roberts [54]. For invariance under choices of analytic data, see Baldwin [6]. Baldwin, Hedden, and Lobb [8] have shown that any Floer-type theory satisfying some mild conditions will support a similar sort of spectral sequence.

2.3.5 The connection between the transverse and contact invariants

Let $K \subset S^3$ be a transverse link in the standard contact structure ξ_{std} . There is a unique lift of ξ_{std} to $S^3(L)$ which we denote by ξ_L . In the paper defining the transverse invariant $\psi(L)$, Plamenevskaya asked whether there is a connection between $\psi(L)$ and $c(\xi_L)$ via the Ozsváth-Szabó spectral sequence. This questions was first answered by Roberts (with elaboration from Baldwin and Plamenevskaya).

Theorem ([55], [9]). *There is an element $x \in E^0(L)$ so that $[x]_2 \in E^2(L)$ equals $[\psi(L)]$ and $[x]_\infty \in E^\infty(L)$.*

Briefly, $\psi(L)$ “converges” to $c(\xi_L)$. This sort of convergence is not of much use on its own; for example, the fact that $[\psi(L)]$ does not imply that $c(\xi_L)$ does, and vice-versa. Still, it suggests that “what’s true for ψ may be true for c ”. Our work in Chapter 4 is motivated by this maxim.

Chapter 3

Branched diagrams and the Ozsváth-Szabó spectral sequence

In this chapter we construct, for any link L with diagram \mathcal{D} , a spectral sequence $E'(\mathcal{D})$ isomorphic to Ozsváth and Szabó's using Heegaard diagrams with a more transparent connection to Khovanov homology. We call these Heegaard diagrams *branched*. Branched diagrams are minimal, in the sense that $E'^0(\mathcal{D}) \cong \widetilde{\text{CKh}}(\mathcal{D})$ as a bigraded vector space.¹ The equality between the ranks of the two vector spaces is obvious from the diagrams, but the gradings depend on the placement of a basepoint in a sensitive way, see Section 3.2.2.

Baldwin has shown that each $E^i(\mathcal{D})$ is a link invariant for $i \geq 2$, so each $E'^i(\mathcal{D})$ is as well [6]. Now let \mathcal{D} be a braid closure diagram for a transverse link in (S^3, ξ) . Let $\psi(\mathcal{D}) \in \text{CKh}(\mathcal{D})$ be Plamenevskaya's transverse element [52]. Baldwin also showed that the image of ψ on each page of E is a transverse invariant, and we obtain the same result for E' . Roberts showed that the image of ψ on E^∞ is naturally identified with the contact element $c(\xi_L) \in \widehat{HF}(-S^3(-L))$, where ξ_L is the lift of ξ to $S^3(-L)$ and c is the Heegaard Floer contact invariant. We can easily identify a generator corresponding to these cycles on a branched diagram. We hope to use this fact to further connect ψ with contact topology.

This chapter is nearly identical to parts of our article “Branched diagrams and the Ozsváth-Szabó spectral sequence”, available on the Arxiv [57].

¹ $E^1(\mathcal{D}) \cong \widetilde{\text{CKh}}(\mathcal{D})$, but $E^0(\mathcal{D})$ will in general have much larger rank than the Khovanov chain complex.

We pursued a spectral sequence from branched diagrams, first suggested to exist in [26], to show that a certain combinatorial spectral sequence defined by Szabó is identical to Ozsváth and Szabó's. However, we find that the face maps in E' are different from Szabó's. The face maps on Szabó's theory Oz are largely determined by a handful of simple linear-algebraic rules. It would be interesting to characterize the maps on E' by similar rules to see exactly how the two theories differ and to produce a combinatorial spectral sequence isomorphic to E' . We speculate some more on this in the final section of the chapter.

3.1 Branched diagrams

In this section we introduce a different set of Heegaard diagrams for the branched double cover of a resolution of a link. They first appeared, in a different guise, in [26].

Let $L \subset S^3$ be a link and \mathcal{D} a diagram for L with c crossings. Draw a small circle around each crossing so that it contains exactly two arcs. For any two resolutions I and I' of \mathcal{D} the diagrams $\mathcal{D}(I)$ and $\mathcal{D}(I')$ differ only within those circles. In S^3 , the links differ only in small balls.

Now let I^0 be the resolution $(0, \dots, 0)$ and consider the diagram $\mathcal{D}(I^0)$. Color the arcs inside the circles blue and add dotted arcs as shown in Figure 3.1. For a component with no crossings, draw a dotted arc to divide it into two pieces and color one side red and the other blue. Now place this diagram on a sphere and make a copy. Properly interpreted, this pair of diagrams is a Heegaard diagram: the dotted arcs are branch cuts connecting the two spheres to form a surface V . The red and blue arcs on each side are connected through the branch cuts to form sets of red and blue circles which we denote by \mathbf{A} and $\mathbf{B}(I^0)$, respectively.

Proposition 3.1.1. *The Heegaard diagram $(V, \mathbf{A}, \mathbf{B}(I^0))$ presents $S^3(\mathcal{D}(I^0))$.*

Proof. Place the diagram $\mathcal{D}(I^0)$, along with the small circles around the crossings, onto a 2-sphere $S \subset S^3$. There are $4k$ points at which the diagram meets the small circles. Leaving those fixed, gently lift the blue curves off of the sphere and push the red curves into it. The two balls bounded by S lift, in the branched cover, to handlebodies with (co)attaching curves \mathbf{A} and \mathbf{B} , respectively. The resulting Heegaard diagram is exactly $(V, \mathbf{A}, \mathbf{B}(I^0))$. \square

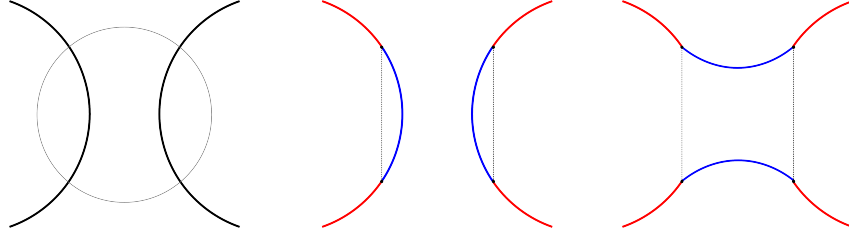


Figure 3.1: On the left, the 0-resolution of a crossing. In the middle, one side of the corresponding local picture on a branched diagram. On the right, the same for the 1 resolution. We have only shown one side of each branched diagram. The other side is identical.

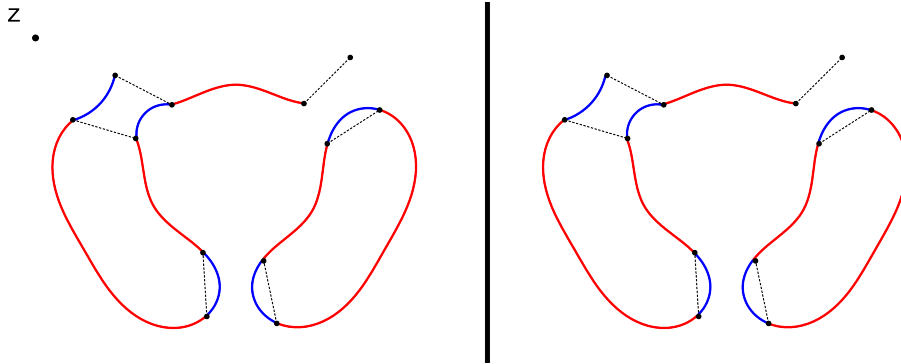


Figure 3.2: A branched diagram from the $(1, 0, 0)$ resolution of a trefoil with the crossings ordered clockwise from the top left. The bar in the middle indicates that the two diagrams lie on different spheres, connected through the branch cuts. The left/top component is marked.

The cautious reader will note that \mathbf{A} and $\mathbf{B}(I^0)$ each have $2k$ elements, but V has genus $2k - 1$. Moreover, the diagram has no basepoint. Choose a pair (a, b) with $a \in \mathbf{A}, b \in \mathbf{B}(I^0)$, $a \cap b \neq \emptyset$; we will assume that the corresponding curves in $\mathcal{D}(I^0)$ border the outermost part of the diagram, but this is not strictly necessary. The diagram $(V, \mathbf{A} \setminus \{a\}, \mathbf{B}(I^0) \setminus \{b\})$ still presents $S^3(\mathcal{D}(I^0))$, and the outermost regions on both sides of diagram are connected. Place a basepoint z in that region. \mathbf{A} and \mathbf{B} will refer to $\mathbf{A} \setminus \{a\}$ and $\mathbf{B} \setminus \{b\}$ for the remainder of this paper, and the diagram $(V, \mathbf{A} \setminus \{a\}, \mathbf{B}(I^0) \setminus \{b\}, z)$ will be denoted by $\mathcal{B}r(I^0)$. The component of $\mathbf{A} \cup \mathbf{B}$ from which curves were removed will be called *marked*.

Let $I \neq I_0$ be a resolution of \mathcal{D} . We define $\mathbf{B}(I)$ by comparison with $\mathbf{B}(I^0)$. At each crossing where I and I^0 determine the same resolution, $\mathbf{B}(I)$ contains curves parallel to those in $\mathbf{B}(I^0)$. At crossings where they disagree, $\mathbf{B}(I)$ contains the green curves in Figure 3.3.

Definition. The Heegaard diagram

$$\mathcal{Br}(I) = (V, \mathbf{A}, \mathbf{B}(I), z)$$

is the *branched diagram* of $D(I)$.

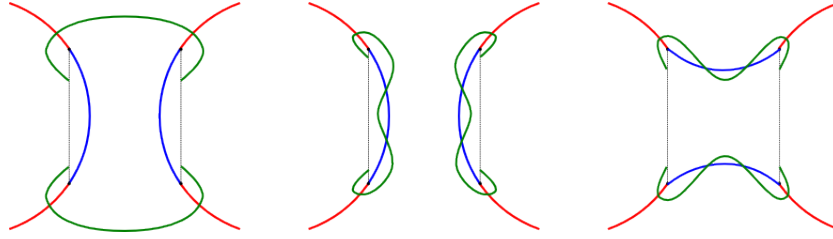


Figure 3.3: Three different local pictures of a branched multidigraph for a change of resolution. On the left, the local picture at the changed resolution. The other pictures are local pictures at unchanged crossings.

Definition. For a path of resolutions \mathbf{I} , the Heegaard multidigraph

$$\mathcal{Br}(\mathbf{I}) = (V, \mathbf{A}, \mathbf{B}(I_1), \dots, \mathbf{B}(I_n), z)$$

is the *branched multidigraph* of \mathbf{I} .

If I' is an immediate successor of I , then $(V, \mathbf{B}(I), \mathbf{B}(I'), z)$ is a standard Heegaard diagram for $\#^{2k-2}(S^2 \times S^1)$. Thus it has a highest degree generator (and cycle) $\Theta_{I_i} \in \widehat{CF}(V, \mathbf{B}(I_i), \mathbf{B}(I_{i+1}), z)$.

3.2 Bouquet diagrams from branched diagrams

Using branched diagrams, we can define a group $X' = \bigoplus_{I \in \{0,1\}^c} \widehat{CF}(\mathcal{Br}(I))$ and a map $D' : X' \rightarrow X'$ by analogy with X and D . It is not clear from the getgo that D' is a differential, much less that the argument from the last chapter produces a spectral sequence isomorphic to Ozsváth and Szabó's. Rather than attempting to adapt their proof, we will show that for every branched (multi)diagram there is a bouquet (multi)diagram which is differs from the branched diagram by a sequence of handleslides. In the next section, we

show that the quasi-isomorphisms of Heegaard Floer chain complexes induced by these handleslides induces an isomorphisms of spectral sequences.²

For \mathcal{D} a diagram of $L \subset S^3$ there is a bouquet diagram closely related to the branched diagram $\mathcal{B}r(I^0)$. The $\mathbf{B}(I^0)$ curves of $\mathcal{B}r(I^0)$ are paired together at crossings of \mathcal{D} . Let $\mathbf{B}'(I^0) \subset \mathbf{B}(I^0)$ be a choice of one such curve at each crossing. The new diagram comes from handlesliding each element of $\mathbf{B}'(I^0)$ over the curve with which it is paired in $\mathbf{B}(I^0)$. Diagrammatically, replace the chosen curve with a circle which contains (in the fixed projection of the diagram) the two branch cuts. Call the collection of such circles \mathbf{C} . Let $\eta(I^0) = \mathbf{C} \cup \mathbf{B}'(I^0)$. For any other resolution I , define $\eta(I) = \mathbf{C} \cup \mathbf{B}'(I)$ as follows: at a 0-resolution, $\mathbf{B}'(I^0)$ and $\mathbf{B}'(I)$ contain the same curves. At a 1-resolution, $\mathbf{B}'(I)$ instead contains a curve which intersects the corresponding curve in $\mathbf{B}'(I^0)$ once and does not intersect any other $\mathbf{B}'(I)$ curves. See Figure 3.4.

Let $\mathcal{B}o(I) = (V, \mathbf{A}, \eta(I), z)$.

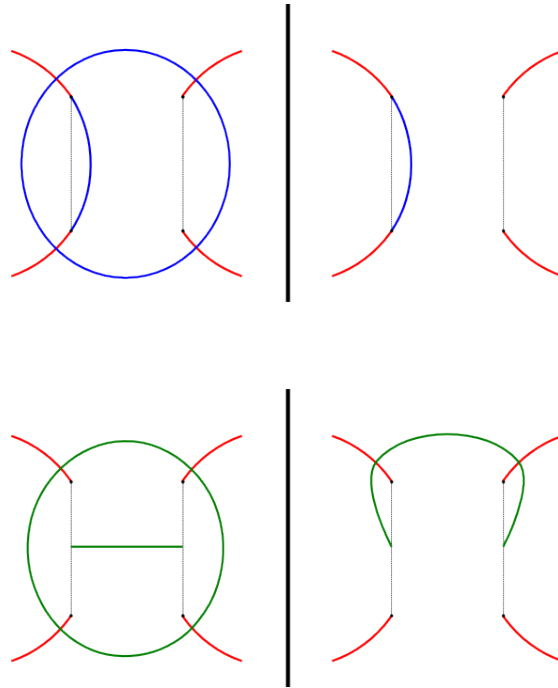


Figure 3.4: On top, both sides of $\mathcal{B}o(I)$ at a 0-resolution. On the bottom, both sides of $\mathcal{B}o(I)$ at a 1-resolution.

²The Heegaard Floer homology of a three-manifold does not depend on the choice of Heegaard diagram: given two diagrams for Y we can always connect them by a series of (pointed) isotopies, handleslides, and (de)stabilizations. These moves induce natural isomorphisms on Heegaard Floer homology groups. But it is not clear *a priori* that they induce isomorphisms of spectral sequences.

Proposition 3.2.1. *The Heegaard diagram $\mathcal{B}o(I)$ presents $S^3(\mathcal{D}(I))$ and is a bouquet diagram for the surgery arcs from the Ozsváth-Szabó construction.*

Proof. The diagram $\mathcal{B}o(I)$ differs from $\mathcal{B}r(I)$ by sliding the C curve over the $\mathbf{B}'(I)$ curve at each crossing, so certainly $(V, \boldsymbol{\alpha}, \boldsymbol{\eta}(I))$ presents $S^3(\mathcal{D}(I))$. The local picture associated to a resolved crossing each has a single curve which intersects the branch cuts. These curves intersect once and do not intersect any other curves, so they lie on a punctured torus on V . They are clearly a meridian and longitude for the lift of the related surgery knot. \square

3.2.1 Admissibility and minimality

We now show that $\mathcal{B}rI$ and $\mathcal{B}oI$ are weakly admissible in the sense of [48]. On each side of $\mathcal{B}r(I)$ there are circles formed by alternating \mathbf{A} and \mathbf{B} curves. Fixing our attention on one side of the diagram, these circles are in one-to-one correspondence with closed components of $\mathcal{D}(I)$, except for the marked component, which corresponds to a line rather than a circle. For a component Q of $\mathcal{D}(I)$, we say a curve γ in \mathbf{A} or \mathbf{B} *belongs to* Q if γ is a subset of Q through this correspondence.

Proposition 3.2.2. *Branched diagrams are weakly admissible.*

Proof. It suffices to show that every periodic domain on $\mathcal{B}r(I)$ has positive and negative coefficients. Let Q_1 be an innermost component of $\mathcal{D}(I)$. There are two regions bounded by the curves belonging to this component, and their difference is a periodic domain P_1 . Now let Q_2 be a component which contains Q_1 and does not contain any other component which contains Q_1 . There are two regions bounded by the curves belonging to Q_1 and the \mathbf{B} curves belonging to Q_0 , and their difference is a periodic domain P_2 . The region obtained by instead using the \mathbf{A} curves belonging to C_0 differs from this one by $\pm P_1$. It is straightforward to extend this method to the remaining components of \mathcal{D} . The result is a linearly independent set \mathbf{P} of $n - 1$ primitive periodic domain, each corresponding to a closed component. Each of these domains has both positive and negative coefficients. The group of periodic domains on $\mathcal{B}r(I)$ is isomorphic to $H^1(S^1 \times S^2; \mathbb{Z}) \simeq \mathbb{Z}^{n-1}$, so \mathbf{P} generates the group. It is clear that any sum of these domains has both positive and

negative coefficients.³

□

We show that bouquet diagrams are admissible by a similar method. Curves \mathbf{A} and $\mathbf{B}'(I) \subset \boldsymbol{\eta}(I)$ may be said to belong to component Q as above, but we will say a curve in C belongs to a component only if its paired curve in $\mathbf{B}'(I^0)$ does not.

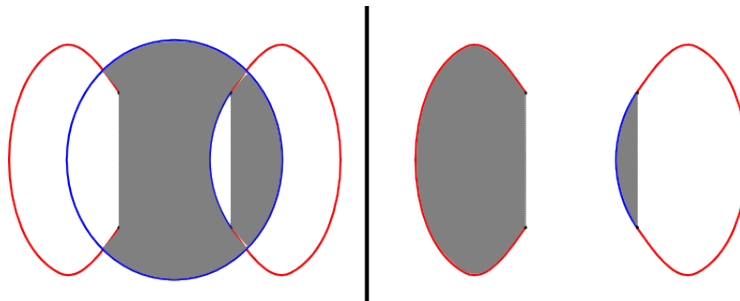


Figure 3.5: A bouquet diagram for the 0-resolution of an unknot. The lightly shaded region is the ‘obvious’ bigon for the left component. The darker region is topologically an annulus, but it can represent a holomorphic disk into the symmetric product of the Heegaard surface by cutting along a \mathbf{A} curve.

Proposition 3.2.3. *Bouquet diagrams are weakly admissible.*

Proof. For each closed component of $\mathcal{D}(I)$, there are two regions bounded by curves belonging to that component. If all the $\boldsymbol{\eta}(I)$ curves belonging to a component are also in $\mathbf{B}'(I)$, then the regions are identical to those in the previous lemma. When a curve in C bounds a region, it is still easy to see how one how it might bound one region. The complementary region is more complicated; an example is shown in Figure 3.5. Again, the difference between these two regions is a periodic domain with positive and negative coefficients. □

Every other Heegaard diagram considered in this chapter consists of some mixture of branched and bouquet diagrams, along with pairs of parallel curves. Using the above arguments it is easy to find a basis of periodic domains with positive and negative coefficients and whose sums must have positive and negative coefficients provided that the parallel curves are properly perturbed.

³The skeptic is encouraged to play the game Lights Out from Tiger Electronics.

3.2.2 Correspondance with Khovanov chain complex

Proposition 3.2.4. *Let $\mathcal{B}r(I)$ be a branched diagram for the resolution I of a diagram for the link L . Only the unique torsion Spin^c structure on $S^1 \times S^2$ is represented by a generator, and $\text{rank } \widehat{CF}(\mathcal{B}r(I)) = \text{rank } \widehat{HF}(\mathcal{B}r(I)) = \text{rank } \widetilde{Kh}(m(L))$.*

Proof. Write \mathfrak{s}_0 for the unique torsion Spin^c structure on $S^1 \times S^2$. As in [47],

$$\text{rank}(\widehat{HF}(\#^n S^1 \times S^2)) = \text{rank}(\widehat{HF}(\#^n S^1 \times S^2, \mathfrak{s}_0)) = 2^n.$$

The Heegaard diagram $\mathcal{B}r(I)$ presents $\#^{n-1} S^1 \times S^2$ where n is the number of connected components of the resolved diagram. Thus it suffices to show that $\text{rank}(\widehat{CF}(\mathcal{B}r(I))) = 2^{n-1}$. A generator of $\widehat{CF}(\mathcal{B}r(I))$ can be written as a choice of one of two orientations of each component of $\mathcal{D}(I)$ except for the marked component. Thus $\text{rank}(\widehat{CF}(\mathcal{B}r(I))) = 2^{n-1}$. In particular, the differential on $\widehat{CF}(\mathcal{B}r(I))$ vanishes.

An explicit correspondance is given as follows: for every pair of parallel curves in $\mathcal{B}r(I)$ there is a pair of intersection points. The one with higher Maslov grading – i.e., the source of the two cancelling disks – corresponds to v_+ , while the other corresponds to v_- . \square

The correspondance depends on the placement of the basepoint z . Without z , it is impossible to determine which generator in $\widehat{CF}(S^1 \times S^2)$ has higher Maslov grading. For more on this point and the trouble it brings, look ahead to 3.4

For a three-manifold Y and a torsion Spin^c structure $\mathfrak{s} \in \text{Spin}^c(Y)$, the group $\widehat{CF}(Y, \mathfrak{s})$ has an (absolute) \mathbb{Q} -valued grading gr defined in [51]. We note here only a few properties of gr . First, for any Heegaard diagram of $S^1 \times S^2$ so that $\widehat{CF}(S^1 \times S^2)$ has exactly two generators, the generators have gradings $1/2$ and $-1/2$, respectively. Second, the grading is compatible with the Künneth formula for Heegaard Floer homology: $\widehat{CF}(Y_1 \# Y_2) \cong \widehat{CF}(Y_1) \otimes_{\mathbb{Z}/2\mathbb{Z}} \widehat{CF}(Y_2)$ is an isomorphism of graded vector spaces. In other words, the grading of a generator in $\widehat{CF}(Y_1 \# Y_2)$ is the sum of gradings of the corresponding generators in $\widehat{CF}(Y_1)$ and $\widehat{CF}(Y_2)$.

In section 2.1 we defined gradings h and q on the Khovanov chain complex. Let $h' :$

$X' \rightarrow \mathbb{Z}$ be defined identically to h . Let $\tilde{q}' = 2 \text{ gr}$, and define $q' : X' \rightarrow X'$ by

$$q'(x) = \tilde{q}'(x) + n_+ - 2n_-.$$

Proposition 3.2.5. *The correspondance in the proof of Proposition 3.2.4 is a graded isomorphism of the vector spaces $X'(\mathcal{D}) \cong \widehat{\text{CKh}}(\mathcal{D})$.*

Proof. Just compare the formulas involved. □

3.3 Handleslides

Let us recap: for a diagram \mathcal{D} with c crossings of a link $L \subset S^3$ we have two groups $X = \bigoplus_{I \in \{0,1\}^c} \widehat{CF}(\mathcal{B}_0(I))$ and $X' = \bigoplus_{I \in \{0,1\}^c} \widehat{CF}(\mathcal{B}_1(I))$. The group X is equipped with a filtered differential D . The group X' is equipped with a filtered map D' , defined identically *mutatis mutandis*. In this section we study the maps induced by the handleslides which transform $\mathcal{B}_0(I)$ to $\mathcal{B}_1(I)$.

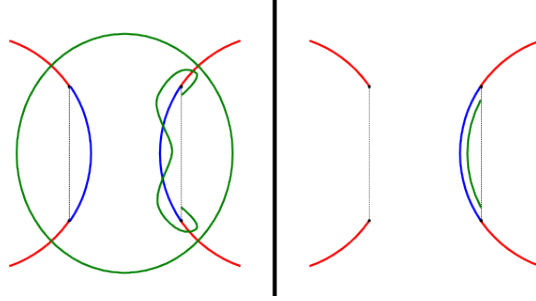


Figure 3.6: A branched multidiagram representing a handleslide at a 0-resolved crossing.

To start, we examine the map induced by the handleslides near the first crossing (the crossings must be ordered to have a cube of resolutions in the first place). As in [54], we may draw and slide parallel curves together. Figure 3.6 shows a Heegaard multidiagram realizing a handleslide at a 0-resolved crossing. The local picture at a 1-resolved crossing is similar. At all other crossings, $\boldsymbol{\eta}(I)$ and $\mathbf{B}(I)$ curves are parallel. For any resolution I the Heegaard diagram $(V, \boldsymbol{\eta}(I), \mathbf{B}(I))$ presents a connected sum of $S^1 \times S^2$ s and $\widehat{CF}(\boldsymbol{\eta}(I), \mathbf{B}(I))$ has a highest degree generator Θ_I . For every path $\mathbf{I} = \{I_1, \dots, I_n\}$ there is a map $\psi_{\mathbf{I}}$ given

on generators by

$$\psi_{\mathbf{I}}(x) = f(x \otimes \Theta_{I_1} \otimes \cdots \otimes \Theta_{I_{n-1}}).$$

Extend the cube of resolutions to $\{0, 1\}^c \times \{0, 1\}$, where the last coordinate specifies whether to use curves from $\mathcal{B}_0(I)$ (for 0) or $\mathcal{B}_1(I)$ (for 1). Let ψ_1 be the map $\psi_1 = \sum \psi_{\mathbf{I}}$ where the sum is taken over paths whose last coordinate changes. (We will freely conflate ψ_1 with the restriction of ψ_1 to a map $X \rightarrow X_1$.) Define maps D_0 and D_1 by

$$D_0 = \sum_{J, J' \in \{0, 1\}^k \times \{0\}} d_{J, J'}$$

$$D_1 = \sum_{J, J' \in \{0, 1\}^k \times \{1\}} d_{J, J'}$$

Note that $D_0|_{X' \times \{0\}} = D$.

Proposition 3.3.1. *The map ψ_1 satisfies $\psi_1 \circ D_0 = D_1 \circ \psi_1$.*

Proof. Let $\phi \in \pi_2(\mathbf{x}, \Theta_{I_1}, \dots, \Theta_{I_{n-1}})$ with $\mu(\phi) = 1$. Write $\mathcal{M}(\phi)$ for the space of holomorphic representatives of ϕ . This space has a compactification whose ends are pairs (ϕ_1, ϕ_2) so that $\phi_1 \star \phi_2 = \phi$ and $\mu(\phi_1) = \mu(\phi_2) = 0$. Here \star is the concatenation operation. More concretely, the ends are “broken polygons” joined at a vertex. Each of these corresponds to a holomorphic polygon with $\mu = 1$ and a degenerating chord, as shown in Figure 3.7. Compactness implies that the sum of the ends must be zero modulo 2. In this schematic, each edge of the polygon is mapped to a set of attaching curves (really, to a torus in a certain symmetric product) and we will abuse notation by identifying the side of the polygon with the curves.

Each polygon counted by ψ_1 has a unique vertex v joining a $\boldsymbol{\eta}$ edge and a \mathbf{B} edge. This vertex, which we call v , represents the handleslide. The character of the degeneration is determined by the position of the degenerating chord relative to v and to the \mathbf{A} edge. Suppose the chord has an endpoint on the \mathbf{A} . The other endpoint must be either to the left or to the right of v , so in the degeneration v ends up in one polygon or the other. The polygon with v is counted by ψ_1 ; it corresponds to a subpath whose last coordinate changes.

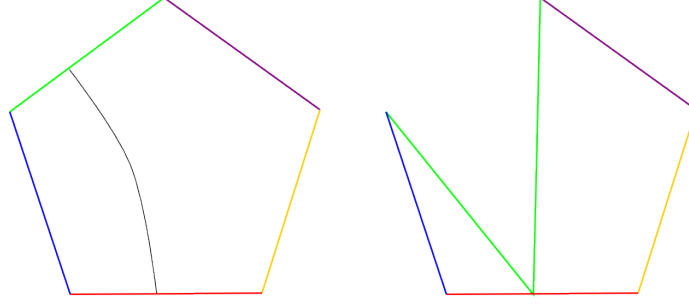


Figure 3.7: A holomorphic pentagon degenerates along a chord into a holomorphic triangle and rectangle. Supposing that the vertex v is where the green and purple edges meet, this degeneration is counted by $\psi_1 \circ D_0$

The other polygon is a component of either D_0 or D_1 . Looking at all degenerations, every component of $\phi_1 \circ D_0$ and $D_1 \circ \psi_1$ appears exactly once. So degenerations along a chord touching the \mathbf{A} edge contribute $\psi_1 \circ D_0 + D_1 \circ \psi_1$ to the boundary sum.

Suppose that the degenerating chord does not have an endpoint on \mathbf{A} and also that it does not separate \mathbf{A} from v . After degenerating, one polygon contains \mathbf{A} and v and the other has edges which live entirely in one cube of resolutions. The cancellation lemma, Lemma 4.5 of [50] or Lemma 7 of [54], shows that the maps counting such polygons sum to zero. The case in which the degenerating chord separates v from \mathbf{A} is the subject of the following lemma. This completes the proof, as it shows that $\psi_1 \circ D + D_1 \circ \psi_1$ is equal to the sum of all the boundary components, and therefore to zero. \square

Lemma 3.3.2. *Let $I, I' \in \{0, 1\}^k \times \{0, 1\}$ be resolutions with differing last coordinates and $I < I'$. Then*

$$\sum_{\text{paths } \mathbf{J} \text{ from } I \text{ to } I'} f_{\mathbf{J}}(\Theta_1 \otimes \cdots \otimes \Theta_n) = 0.$$

Proof. Our argument closely follows those in [50] and [54]. Suppose that $n > 2$. We will show that any element of $\pi_2(\Theta_1, \dots, \Theta_n)$ has positive Maslov index.

One may construct a polygon counted in the sum by splicing together several triangles. There are three sorts of constituent triangles:

1. those of the form $(\boldsymbol{\eta}(J_0), \boldsymbol{\eta}(J_i), \boldsymbol{\eta}(J_{i+1}))$
2. those of the form $(\boldsymbol{\eta}(J_0), \mathbf{B}(J_j), \mathbf{B}(J_{j+1}))$

3. a single triangle of the form $(\boldsymbol{\eta}(J_0), \boldsymbol{\eta}(J_k), \mathbf{B}(J_{k+1}))$.

The third type contains the vertex v . Every triple of the first type presents a surgery cobordism between connected sums of $S^1 \times S^2$ s. Any contributing triangle must have Maslov index zero, so the corresponding map sends the highest degree generator in $\widehat{CF}(\boldsymbol{\eta}(J_0), \boldsymbol{\eta}(J_i)) \otimes \widehat{CF}(\boldsymbol{\eta}(J_i), \boldsymbol{\eta}(J_{i+1}))$ to the highest degree generator in $\widehat{CF}(\boldsymbol{\eta}(J^0), \boldsymbol{\eta}(J^{i+1}))$, see Lemma 3 in [54]. To obtain an honest polygon we must ‘undo’ the degenerations, increasing the Maslov index by one each time. There must be at least one triangle of type 1 or 2 if $n > 2$, so every polygon has Maslov index greater than 0. As all the Θ s live in torsion Spin^c structures, the addition of a doubly-periodic domain does not affect its Maslov index. It follows that no such polygon has Maslov index zero. An identical argument applies to triples of the second sort.

If $n = 1$ then the lemma is simply that Θ is a cycle. In the case $n = 2$, the map $f_{\mathbf{J}}$ counts certain triangles in which one vertex is v . These correspond to changes of codes of the form $(0, \dots; 0) \rightarrow (1, \dots; 0) \rightarrow (1, \dots; 1)$ or $(0, \dots; 0) \rightarrow (0, \dots; 1) \rightarrow (1, \dots; 1)$. In each case there is a unique triangle connecting highest degree generators, see Figure 3.8. The triangles shown have Maslov index according to Sarkar’s formula in Section 2.3.3. An analysis of periodic domains shows that there are no other triangles between the highest degree generators. The remaining curves in the diagram come in parallel triples. \square

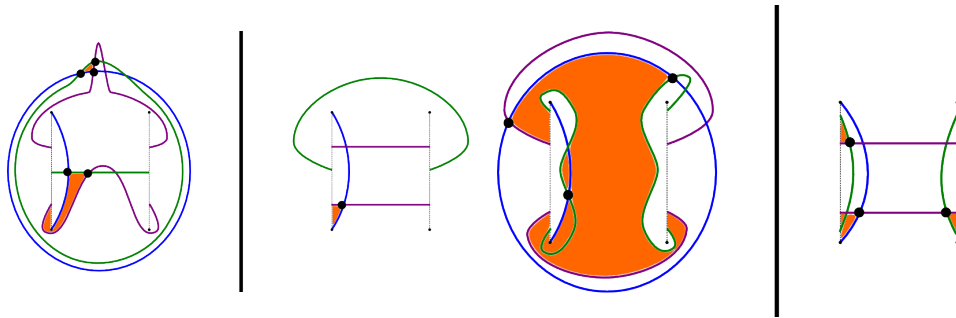


Figure 3.8: The \mathbf{B} curves for the paths $(0, \dots; 0) \rightarrow (1, \dots; 0) \rightarrow (1, \dots; 1)$ (left) and $(0, \dots; 0) \rightarrow (0, \dots; 1) \rightarrow (1, \dots; 1)$ (right). The intersection points constituting the highest degree generator are marked with circles. The shaded region is the region of the unique holomorphic triangle connecting the generators.

This argument works just as well if we change a second crossing after changing the first, and so on. Let X_i be the group obtained by doing i of these handleslides. Let D_i be the

putative differential on X_i , and let $\psi_{i+1} : X_i \rightarrow X_{i+1}$ be the map induced by the next handleslide. Let $\Psi = \psi_n \circ \dots \circ \psi_1$ and write $\phi_i : X_i \rightarrow X_{i-1}$ for maps defined identically to ψ_i but induced by the reverse handleslide. Let $\Phi = \phi_1 \circ \dots \circ \phi_n$.

Lemma 3.3.3. *The pair (X', D') is a filtered complex.*

Proof. Suppose \mathcal{D} has n crossings so that $X = X_n = \Phi(X')$. By definition $D_n = D$. Proposition 3.3.1 implies that the maps Ψ and Φ are D - D' -equivariant so $\Phi \circ D'^2 = D^2 \circ \Phi = 0$. Let ϕ_i^0 be the component of ϕ_i which only counts paths of length two (i.e. holomorphic triangles). Let $\Phi^0 = \phi_2^0 \circ \dots \circ \phi_n^0$ so that Φ^0 is a direct sum of maps $\Phi_I^0 : \widehat{CF}(\mathcal{B}r(I)) \rightarrow \widehat{CF}(\mathcal{B}o(I))$. The proof of topological invariance of Heegaard Floer homology shows that each of these maps is a quasi-isomorphism. Now Lemma 3.2.4 implies that Φ^0 is injective: if $\text{rank}(\phi_I^0) < \dim(\widehat{CF}(\mathcal{B}r(I)))$, then $\text{rank}((\phi_I^0)_*) < \dim(\widehat{CF}(\mathcal{B}r(I))) = \dim(\widehat{HF}(\mathcal{B}r(I)))$ and Φ_I^0 could not be a quasi-isomorphism.

For the sake of contradiction, suppose that $(D')^2(\mathbf{x}) \neq 0$ for some $\mathbf{x} \in X$. Then $(D')^2(\mathbf{x})$ may have components in several direct summands. Say that the *weight* of a resolution is the sum of its entries. Let x_0 be a non-zero component of $(D')^2(\mathbf{x})$ in a direct summand whose resolution I_0 has lowest possible weight. Then $\Phi \circ (D')^2(\mathbf{x})$ has a component $\Phi^0 \circ (D')^2(\mathbf{x}) \neq 0$ in $\widehat{CF}(\mathcal{B}o(I_0))$. Because x_0 is in the lowest possible weight, no other component of Φ can cancel with Φ^0 , so $\Phi \circ (D')^2(\mathbf{x}) \neq 0$. This contradiction implies that $(D')^2 = 0$. \square

Now we are able to complete the proof of the theorem stated in the introduction.

Theorem 3.3.4. *Let $L \subset S^3$ be a link with diagram \mathcal{D} . Let $E'(\mathcal{D})$ be the spectral sequence induced by the order filtration on (X', D') and let $E(\mathcal{D})$ be the Ozsváth-Szabó spectral sequence. Then $E^k(\mathcal{D}) \cong E'^k(\mathcal{D})$ for $k \geq 1$.*

Proof. The map Ψ is a filtered chain map, so it induces a map of spectral sequences. The induced map on E^1 is the direct sum of handleslide maps $\widehat{HF}(\mathcal{B}o(I)) \rightarrow \widehat{HF}(\mathcal{B}r(I))$ which are shown to be isomorphisms in the proof of the topological invariance of Heegaard Floer homology. This implies that the maps induced by Ψ are isomorphisms for $k \geq 1$, see Theorem 3.4 in [43]. \square

For a transverse link $L \subset (S^3, \xi)$ with braid closure diagram $\bar{\beta}$, let $\psi(\bar{\beta}) \in \text{CKh}(\bar{\beta})$ be Plamenevskaya's transverse element in Khovanov homology [52].

Corollary 3.3.5. *The vector spaces $E^k(L)$ are smooth link invariants for $k \geq 2$. The image $[\psi(\bar{\beta})] \in E^k(\bar{\beta})$ is a transverse link invariant for $k \geq 2$.*

Proof. In [6], Baldwin shows that $E^k(L)$ is a (smooth) link invariant for $k \geq 2$ and that the image of $\psi(L)$ on $E^k(L)$ is a transverse invariant for $k \geq 2$. The proofs of these facts translate to the branched setting. The essential point is that if \mathcal{D} and \mathcal{D}' are diagrams of L , any sequence of Reidemeister moves induces a map $X'(\mathcal{D}) \rightarrow X'(\mathcal{D}')$ which in turn induces an isomorphism on E'^2 . Theorem 3.4 in [43] implies that the two spectral sequences are isomorphic.

For the second statement, we use the fact that $\psi(\bar{\beta})$ has lowest annular grading among all elements of the Khovanov complex of the closure of an annular link [55]. It is not hard to see that the differential D' does not increase this grading as in [55] and [26]. \square

More concretely, if $\bar{\beta}$ is a braid closure diagram for the transverse link $L \subset (S^3, \xi)$, it is easy to spot $\psi(\bar{\beta})$ in $\mathcal{Br}(\bar{\beta})$: simply look in the unique braidlike resolution and find the Heegaard Floer generator with lowest grading. Work of Roberts [55] shows that this same generator represents the Heegaard Floer contact invariant $c(\xi_L) \in \widehat{HF}(\mathfrak{S}^3(-L))$ for the contact structure ξ_L which lifts ξ .

3.4 Comparison with Szabó's spectral sequence

In [61], Szabó defines a new spectral sequence from reduced Khovanov homology. Let $L \subset S^3$ be a link with a marked, spherical diagram \mathcal{D} . Let $\text{COz}(\mathcal{D}) = \text{CKh}(\mathcal{D})$ as a vector space. Define $\partial_1 : \text{COz}(\mathcal{D}) \rightarrow \text{COz}(\mathcal{D})$ to be the usual Khovanov differential. Now consider a k -dimensional face of the cube. The lowest and highest weight resolutions of the face differ by k changes of resolution which may be encoded by k arrows. We call these arrows *decorations*. The lowest weight diagram along with these decorations is called a *k-dimensional configuration*. Some subset of the closed components meet the decorations; these components are called *active circles*. The remaining components are called *passive*

circles. The circles in the lowest weight resolution are called *starting circles* and the circles in the highest weight diagram are called *ending circles*. Szabó defines a map across the face which depends on the configuration. Write ∂_k for the sum of these maps defined across k -dimensional faces. (The exact form of these maps can be found in [61].) Write $\text{Oz}(\mathcal{D})$ for the homology of $\text{COz}(\mathcal{D})$.

Theorem (Szabó). $(\text{COz}(\mathcal{D}), \partial_1 + \partial_2 + \dots)$ is a complex, and its homology $\text{Oz}(\mathcal{D})$ is a link invariant.

Write $\partial_{\text{Oz}} = \partial_1 + \partial_2 + \dots$. This map is characterized by the several rules. Let C be a k -dimensional configuration and let F_C be the map assigned to C .

- *Disconnected configurations*: if the union of the active circles and their decorations is disconnected, then $F_C = 0$.
- *Extension*: on tensor factors corresponding to passive circles, F_C acts as the identity.
- *Grading*: $q(F_C(x)) - q(x) = k - 2$.
- *Reversal*: The map F_C is the same as the map assigned to $r(C)$, the configuration with oppositely oriented decorations.
- *Naturality*: Let $\phi: S^2 \rightarrow S^2$ be a diffeomorphism. Then $F_{\phi(C)} = F_{\phi(C)}$, identifying closed components of C and C' via ϕ .
- *Duality*: Write C_0 for the starting circles and C_1 for the ending circles. There is a dual configuration C^* from C_1 to C_0 whose decorations are the images of the decorations of C under surgery. Let $m(C^*)$ be the same configuration but on an oppositely oriented sphere. There is a duality map on Khovanov homology which sends $v_+ \rightarrow v_-$ and $v_- \rightarrow v_+$. Let x be a generator of $\widetilde{\text{CKh}}(C_0)$ and y a generator of $\widetilde{\text{CKh}}(C_1)$. Then the coefficient of $F_C(x)$ on y is equal to the coefficient of $F_{m(C^*)}(y^*)$ at x^* .
- *Basepoint action and filtration*: Let $p \in \mathcal{D}$. Let $x_p: \text{CKh}(\mathcal{D}) \rightarrow \text{CKh}(\mathcal{D})$ be the basepoint map. Then $F_C \circ x_p = x_p \cdot F_C$.

These rules appear to be related to properties of Heegaard Floer homology. For example, the last rule is analogous to the fact that Heegaard Floer polygon maps are $\mathbb{Z}/2\mathbb{Z}[U]$ -module maps. The first rule corresponds to the *grading conjecture* that there is a grading on the Ozsváth-Szabó spectral sequence so that the differential on E^k acts with grading $2 - k$. The

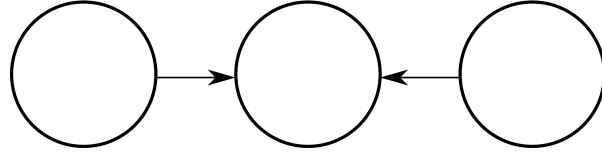


Figure 3.9: Configuration 2 in Szabó's labeling.

basepoint rule allows us to define a reduced theory, $\widetilde{\text{COz}}$.

To see how these rules determine the maps, consider the configuration C_2 in Figure 3.9. Suppose that \mathcal{F}_{C_2} is not zero. By extension and naturality, the map is determined by this local picture. Let t be a simple tensor in $\widetilde{\text{CKh}}(C_2)$ in which one of the circles is labeled v_- . The filtration rule implies that $\mathcal{F}_{C_2}(t) = v_-$. The grading rule then implies that exactly two of the active components is v_- -labeled. A similar argument shows that $\mathcal{F}_{C_2}(t) = 0$ if more or fewer of the components are labeled v_- . Finally, naturality implies that the outer two components must be the v_- -labeled ones because there is a diffeomorphism of S^2 which reverses their roles in the picture.

Based on structural similarities and Seed's computations [59], Seed and Szabó conjecture the following.

Conjecture ([59, 61]). $\widetilde{\text{Oz}}(L) \cong \widehat{\text{HF}}(\Sigma(L))$, and the spectral sequence from $\widetilde{\text{COz}}(\mathcal{D})$ to $\widehat{\text{HF}}(\Sigma(L))$ is isomorphic to the Ozsváth-Szabó spectral sequence.

We initially pursued Theorem 3.3.4 in the hope of showing that $E'(\mathcal{D})$ agrees with $\text{Oz}(\mathcal{D})$ or, more optimistically, that $\text{Oz}(\mathcal{D}) \cong X'(\mathcal{D})$. The latter is not true in general. Consider the configuration C_1 shown in Figure 3.10. Figure 3.11 shows the corresponding branched diagram.⁴ If $\text{Oz}(\mathcal{D})$ were identical to $X'(\mathcal{D})$ there would be a single (mod 2) holomorphic quadrilateral representing the map F_{C_1} , which maps $v_+ \otimes v_+$ to $v_+ \otimes v_+$. Figure 3.12 shows that there are no such quadrilaterals: the region corresponding to such a quadrilateral would differ from the region shown by a periodic domain, and the resulting domain would have negative coefficients. In fact, the only non-zero component of the Heegaard Floer map from the multidiagram in Figure 3.11 sends $v_+ \otimes v_+$ to $v_+ \otimes v_-$, where in the latter tensor

⁴We could also consider the case in which part of C_1 is the marked component. The analysis is identical.

product the labeling of the outer circle comes first.

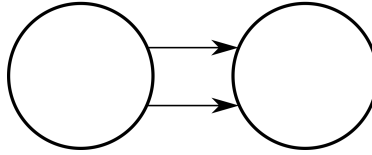


Figure 3.10: Configuration 1 in Szabó's labeling.

As noted at the end of Section 3.2.2, the correspondance between Floer and Khovanov generators is determined by the basepoint z of the underlying branched diagrams. Moving the basepoint across a curve flips the gradings of the generators corresponding to labelings of any component containing that curve. There is a basepoint placement in Figure 3.12 so that the quadrilateral map agrees with F_{C_1} .

Similar examinations of the other configurations suggests that the discrepancy between X' and Oz stems from the spherical symmetry in Oz which is broken by the placement of a basepoint in X' . In Oz , the two ending circles of configuration 1 are indistinguishable, and in fact they may be isotoped to appear unnested in a planar diagram. This is not possible in the Heegaard Floer world. The Heegaard Floer triangle maps agree with the maps on Oz in configurations like configuration 2 in which circles are not nested.

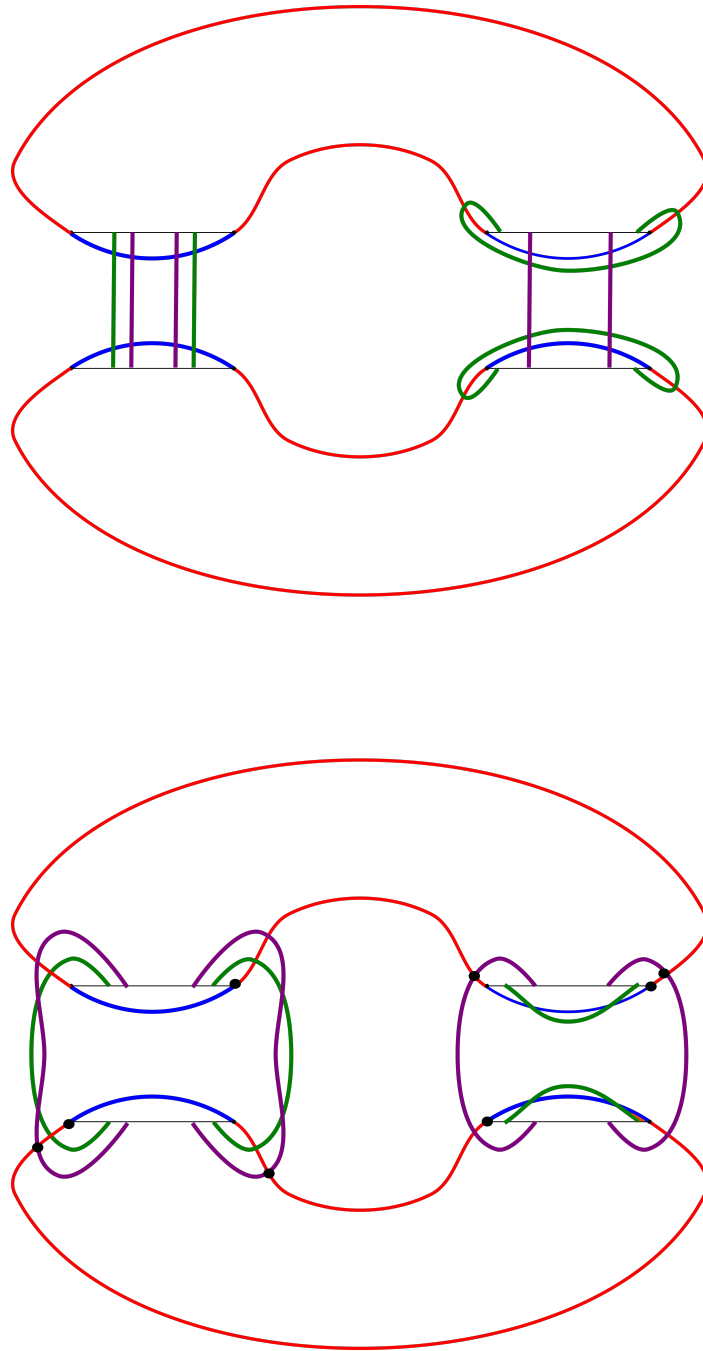


Figure 3.11: The branched Heegaard multidiagram from configuration 1. The black (resp. grey) dots mark intersection points which belong to the Heegaard Floer generators corresponding to $v_+ \otimes v_+$ on the starting (resp. ending) circles.

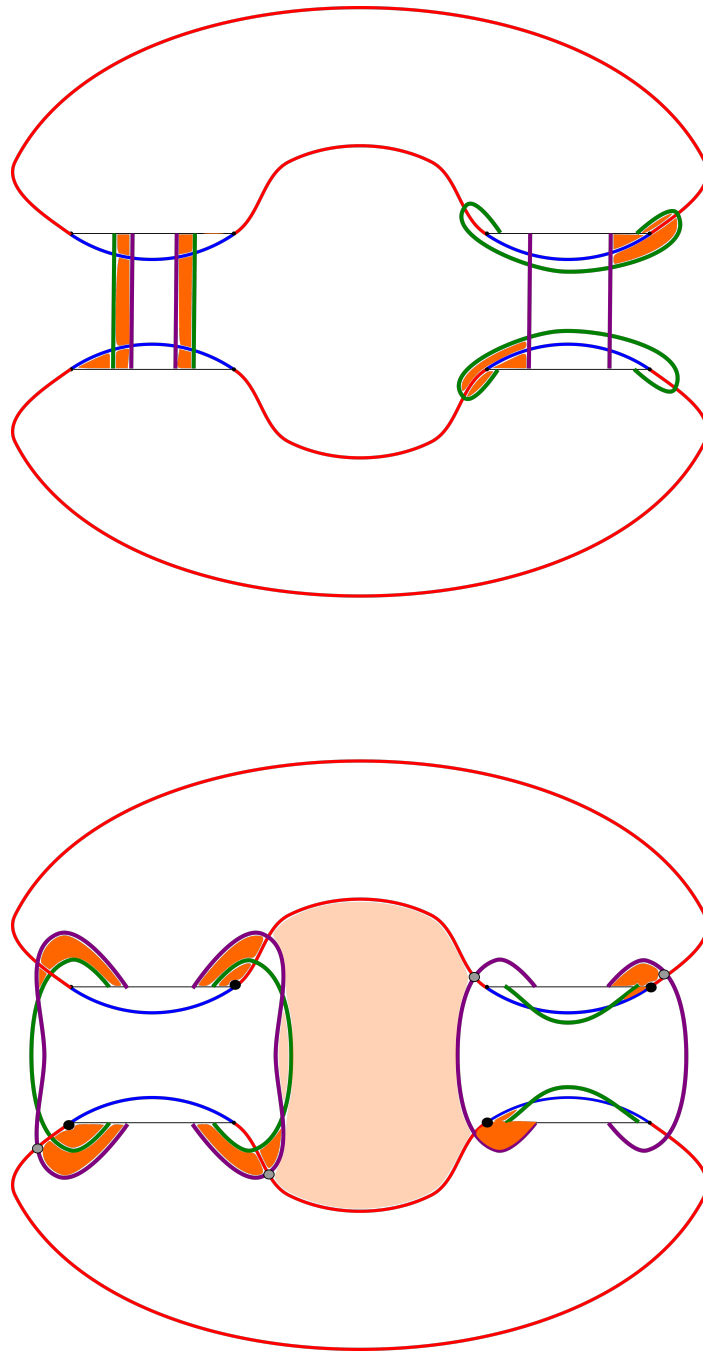


Figure 3.12: A region corresponding to a Whitney quadrilateral. The orange regions have coefficient $+1$ and the negative regions have coefficient -1 .

Chapter 4

An annular refinement of the transverse invariant in Khovanov homology

Given a link L equipped with an embedding into a thickened annulus (i.e. $L \subset A \times I \subset S^3$), its Khovanov chain complex can be endowed with an additional grading called the k -grading, first studied in [4] and [55]. For a resolution with a single component, $k(v_{\pm}) = \pm 1$ if the component is not null-homotopic in $A \times I$, and $k(v_{\pm}) = 0$ otherwise. We extend the grading to tensor products by summation. The Khovanov differential is non-increasing in the k -grading, so k induces a filtration on the Khovanov complex. The homology of the associated graded chain complex is called *annular Khovanov homology*, denoted here as $\text{AKh}(L)$ (elsewhere also called *sutured annular Khovanov homology* or *sutured Khovanov homology* and denoted $\text{SKh}(L)$). AKh is an invariant of annular links and not a transverse invariant. For a braid closure $\bar{\beta}$, the element $\psi(\bar{\beta}) \in \text{CKh}(\bar{\beta})$ is the unique element with lowest k -grading.

Standard algebraic machinery (see [31] for an introduction and [43] for a thorough treatment) produces a spectral sequence from the associated graded object of a filtered

The work in this chapter is joint with Diana Hubbard. It is identical except for some minor changes to [29], to be published in *Algebraic & Geometric Topology*, published by *Mathematical Sciences Publishers*.

complex to the homology of that complex and therefore from AKh to Kh. Our original goal in this chapter was to define a (perhaps effective) transverse invariant by exploring the behavior of Plamenevskaya's class in this spectral sequence. AKh is known to distinguish some braids whose closures are smoothly isotopic but not transversely isotopic (see [28]), and so it is natural to suspect that the spectral sequence from AKh to Kh also captures non-classical information.

For a braid β with closure $\bar{\beta}$, write $\mathcal{F}_i(\bar{\beta}) = \{x \in \text{CKh}(\bar{\beta}) : k(x) \leq i\}$.

Definition 4.0.1. Let β be an n -strand braid with closure $\bar{\beta}$ and suppose that $\psi(\bar{\beta})$ is a boundary in $\text{CKh}(\bar{\beta})$. Define

$$\kappa(\beta) = n + \min\{i : [\psi(\bar{\beta})] = 0 \in H(\mathcal{F}_i)\}.$$

If $\psi(\bar{\beta})$ is not a boundary then define $\kappa(\beta) = \infty$.

The function $\kappa: B_n \rightarrow \mathbb{Z}$ is only a conjugacy class invariant rather than a transverse invariant.

Theorem 4.0.1. κ is an invariant of conjugacy classes in the braid group B_n . It may increase by 2 under positive stabilization and is thus not a transverse invariant.

Nevertheless, κ can distinguish conjugacy classes of some braids whose closures are transversely non-isotopic but have the same classical invariants.

Proposition 4.0.2. For any $a, b \in \{0, 1, 2\}$, the pair of closed 4-braids

$$A(a, b) = \sigma_3 \sigma_2^{-2} \sigma_3^{2a+2} \sigma_2 \sigma_3^{-1} \sigma_1^{-1} \sigma_2 \sigma_1^{2b+2} \quad \text{and}$$

$$B(a, b) = \sigma_3 \sigma_2^{-2} \sigma_3^{2a+2} \sigma_2 \sigma_3^{-1} \sigma_1^{2b+2} \sigma_2 \sigma_1^{-1},$$

related by a negative flype, can be distinguished by κ : indeed, $\kappa(A(a, b)) = 4$ and $\kappa(B(a, b)) = 2$. For any pair (a, b) , the braids $A(a, b)$ and $B(a, b)$ are transversely non-isotopic but have the same classical invariants [33].

Lipshitz, Ng, and Sarkar, using a filtered refinement of $\psi(L)$ valued in the Lee–Bar-Natan deformation of Khovanov homology, showed that Plamenevskaya's class is invariant

under negative flypes [41]. The above proposition could be seen as evidence that κ carries non-classical information even if ψ does not.

κ has nice properties mirroring those of ψ , and our calculations have some interesting consequences. In Section 4.3 we collect these observations. In particular, we show using Proposition 4.0.2 that the spectral sequence from AKh to Kh does not necessarily collapse immediately, providing a counterexample to Conjecture 4.2 from [30]. In addition, our work together with that of Baldwin and Grigsby in [7] provides a solution (faster than that of [7]) to the word problem for braids.

The behavior of κ under positive stabilization provided some promise that a reduced analogue of κ might be a transverse invariant. In Section 4.4 we define κ for both versions of reduced Khovanov homology. However, these constructions depend on the placement of the basepoint. We still have some hope that these reduced constructions will provide non-classical transverse information. In any case, the fact that the two reduced variants are apparently independent demonstrates that the two reductions of Khovanov homology are quite different with respect to the k -grading.

This project was inspired by similar constructions in Floer homology. Let (Y, ξ) be a contact three-manifold. Recall that there are elements $c_\xi \in \widehat{HF}(Y)$ and $\emptyset_\xi \in ECH(Y)$ (embedded contact homology) which are invariants of ξ . It is known that each of these elements vanishes if (Y, ξ) is overtwisted ([49], [17]) or if (Y, ξ) contains *Giroux n -torsion* for any $n > 0$ ([22]) (both converses are false). In [38], Latschev and Wendl study *algebraic torsion* in symplectic field theory and show that it can obstruct fillability. Hutchings adapts this work to embedded contact homology by constructing a relative filtration on $ECH(Y)$. He defines the algebraic torsion of the contact element to be the lowest filtration level at which \emptyset_ξ vanishes. As ECH is known to be isomorphic to \widehat{HF} (see [39]) by an isomorphism carrying \emptyset_ξ to c_ξ , it is reasonable to suspect that there is an analogous construction in Heegaard Floer homology. This is the subject of ongoing work by Baldwin and Vela-Vick [5] and independently by Kutluhan, Matic, Van-Horn Morris, and Wand [37].

Now let $L \subset (S^3, \xi)$ be a transverse link. The branched double cover $\Sigma(L)$ inherits a contact structure $\xi(L)$ from (S^3, ξ) . Plamanevskaya conjectured [52] and Roberts proved [55] (see also [9]) that $\psi(L)$ “converges” to $c_{\xi(L)}$ in the Ozsváth-Szabó spectral sequence in

the sense that there is some $x \in E^0(L)$ so that $[x]_2 = \psi(L) \in E^2(L)$ and $[x]_\infty = c_{\xi(L)} \in E^\infty(L)$. This is a weak sort of convergence – in particular, the vanishing or non-vanishing of the two elements are independent – but it has been used fruitfully, e.g. [9]. We hope to use this connection to derive contact-theoretic information from κ .

4.1 The annular filtration

Let $A \subset \mathbb{R}^2$ be a standard annulus in \mathbb{R}^2 . An *annular link* is a link $L \subset A \times [0, 1]$. Let γ be a simple closed curve from the inner boundary of $A \times \{\frac{1}{2}\}$ to the outer boundary. Let $\pi: A \times I \rightarrow A$ be the projection. Let L be an annular link with diagram \mathcal{D} . A component C of the resolved diagram is called *trivial* if the mod 2 intersection number of $\pi(C)$ with $\pi(\gamma)$ is 0 and is called *non-trivial* otherwise. The k -grading of a generator x is

$$k(x) = \#\{\text{non-trivial circles in } x \text{ labeled } v_+\} \\ - \#\{\text{non-trivial circles in } x \text{ labeled } v_-\}.$$

Roberts [55], following [4], shows that the Khovanov differential is non-increasing in k . Thus the subcomplexes $\mathcal{F}_i(\mathcal{D}) = \{x \in \text{CKh}(\mathcal{D}) : k(x) \leq i\}$ form a bounded filtration of $\text{CKh}(L)$. Moreover, the filtered chain homotopy type of $\text{CKh}(\mathcal{D})$ is an invariant of L as an annular link. For a filtered complex (X', d', \mathcal{F}'_i) the *associated graded object* is the direct sum of complexes $\bigoplus_i \mathcal{F}'_i / \mathcal{F}'_{i-1}$. There is a spectral sequence from the associated graded object to the homology of the total complex, see [43]. The associated graded object of the Khovanov chain complex filtered by k is called *annular Khovanov homology* and is denoted by $\text{AKh}(L)$. Roberts concludes the following.

Theorem 4.1.1. [55] *For any annular link L there is a spectral sequence from $\text{AKh}(L)$ to $\text{Kh}(L)$.*

Braid closures may be naturally regarded as annular links, and annular Khovanov homology has proven to be a powerful tool in studying braids. See, for example, [26], [7], [25], and [28].

4.2 Definition and invariance of κ

Let $\beta \in B_n$ be a braid with transverse element $\psi(\bar{\beta})$. The k -filtration on $\text{CKh}(\bar{\beta})$ has the form

$$0 \subset \mathcal{F}_{-n} \subset \mathcal{F}_{2-n} \subset \cdots \subset \mathcal{F}_{n-2} \subset \mathcal{F}_n = \text{CKh}(\bar{\beta})$$

where \mathcal{F}_{-n} is generated by $\psi(\bar{\beta})$, so $\psi(\bar{\beta}) \in \mathcal{F}_i$ for $i \geq -n$. We restate Definition 4.0.1:

Definition. Let $\beta \in B_n$ and suppose that $\psi(\bar{\beta})$ is a boundary in $\text{CKh}(\bar{\beta})$. Define

$$\kappa(\beta) = n + \min\{i : [\psi(\bar{\beta})] = 0 \in H(\mathcal{F}_i)\}.$$

If $\psi(\bar{\beta})$ is not a boundary, then define $\kappa(\beta) = \infty$.

We will say that $y \in \text{CKh}(\bar{\beta})$ realizes $\kappa(\beta)$ if $dy = \psi(\bar{\beta})$ and $k(y) = \kappa(\beta) - n$. Note that κ is always even and that $2 \leq \kappa(\beta) \leq 2n$. The only element with k -grading n is the all v_+ labeling of the braidlike resolution, so in fact $\kappa(\beta) \leq 2(n-1)$. We now show that κ is a well-defined function on B_n . First, an algebraic lemma.

Lemma 4.2.1. *Let (X, d, \mathcal{F}) and (X', d', \mathcal{F}') be complexes with bounded filtrations, and suppose that $f: X \rightarrow X'$ is a filtered chain map. For any non-zero cycle $x \in X$, define $\kappa(x) = \min\{i : [x] = 0 \in H_*(\mathcal{F}_i)\}$ or $\kappa(x) = \infty$ if x is not a boundary. Define κ' analogously on X' . Suppose that $f(x) = y \neq 0$. Then $\kappa(x) \geq \kappa'(y)$. If there is a filtered chain map $g: X' \rightarrow X$ with $g(y) = x$, then $\kappa(x) = \kappa'(y)$.*

Proof. Chain maps carry cycles to cycles, so if $\kappa(x)$ is defined then so is $\kappa'(y)$. There is nothing left to prove if $\kappa(x) = \infty$, so suppose that $\kappa(x)$ is finite. Then there is some $w \in \mathcal{F}_{\kappa(x)}$ so that $dw = x$, and $(f \circ d)(w) = y = (d \circ f)(w)$. As f is filtered, $f(w) \in \mathcal{F}'_{\kappa(x)}$, so $\kappa'(y) \leq \kappa(x)$. If there is a filtered chain map g with $g(y) = x$, then the opposite inequality shows that $\kappa(x) = \kappa'(y)$. \square

The κ of Lemma 4.2.1 differs from that of Definition 4.0.1 in that the latter is normalized using the braid index, but the lemma clearly still applies to the Definition.

Proposition 4.2.2. *Suppose that β and β' are words in the Artin generators so that $\beta = \beta'$ in B_n . Then $\kappa(\beta) = \kappa(\beta')$.*

Proof. It will suffice to show that $\kappa(\beta)$ is invariant under Reidemeister 2 and Reidemeister 3 moves which do not cross the braid axis. These moves induce natural maps on the Khovanov chain complex which carry $\psi(\beta)$ to $\psi(\beta')$, see [52]. For a digestible summary of these maps, see [11]. If these maps are filtered, then Lemma 4.2.1 completes the proof.

The map induced by Reidemeister 2 (and its inverse) is a direct sum of identity maps and compositions of saddles with cups and caps. The saddles, cups, and caps do not cross the braid axis. Certainly the identity map is filtered. One may check directly that saddle maps are filtered; alternatively, observe that a saddle may be viewed as a component of the Khovanov differential of some annular link and so it must be filtered. Cups and caps that do not cross the braid axis cannot change the k -grading. Thus the Reidemeister 2 map is filtered. An identical analysis shows that the Reidemeister 3 maps are filtered. \square

Considering braids instead of their closures, we obtain the following.

Proposition 4.2.3. *κ is an invariant of conjugacy classes in B_n .*

A program to compute κ is available at www2.bc.edu/adam-r-saltz/kappa.html.

4.3 Examples and Properties of κ

4.3.1 Main example

An immediate first question is whether elements in k -grading $-n + 2$ always suffice to kill $\psi(\bar{\beta})$ whenever $[\psi(\bar{\beta})] = 0$, that is, whether $\kappa = 2$ for all braids with $[\psi(\bar{\beta})] = 0$. Proposition 4.0.2, using examples from Theorem 1.1 in [33], shows that this is false. We restate it here:

Proposition. *For any $a, b \in \{0, 1, 2\}$, the pair of closed 4-braids*

$$A(a, b) = \sigma_3 \sigma_2^{-2} \sigma_3^{2a+2} \sigma_2 \sigma_3^{-1} \sigma_1^{-1} \sigma_2 \sigma_1^{2b+2} \quad \text{and}$$

$$B(a, b) = \sigma_3 \sigma_2^{-2} \sigma_3^{2a+2} \sigma_2 \sigma_3^{-1} \sigma_1^{2b+2} \sigma_2 \sigma_1^{-1},$$

related by a negative flype, can be distinguished by κ : indeed, $\kappa(A(a, b)) = 4$ and $\kappa(B(a, b)) = 2$.

Proof. By computation. □

We do not know if this relation holds for all $a, b \in \mathbb{Z}_{\geq 0}$. As $\overline{A}(a, b)$ and $\overline{B}(a, b)$ are in the same isotopy class, they have isomorphic Khovanov homologies. Still, annular Khovanov homology can differentiate them (see [28]) for $a, b \in \{0, 1, 2\}$.

4.3.2 Negative Stabilization

Proposition 4.3.1. *If a closed n -braid β is a negative stabilization of another braid, then $\kappa(\beta) = 2$.*

Proof. In Theorem 3 of [52], Plamenevskaya constructs an element $y \in CKh(\beta)$ such that $dy = \psi(\beta)$ as follows: consider the resolution formed from taking the 0-resolution of the negative crossing from the negative stabilization, the 1-resolution for all other negative crossings, and the 0-resolution for all positive crossings. The element y is obtained by assigning each circle in this resolution v_- . It is clear that y has k -grading $-n + 2$. □

4.3.3 Positive Stabilization

Define an *arc* of a closed braid diagram to be a segment of the link that goes from one crossing to another crossing without traversing over or under any other crossings. An *innermost arc* is one for which we can draw a straight line from the braid axis to any point on the arc without crossing any other arcs. An *innermost point* is a point lying on an innermost arc.

Given an n -strand braid β , we define $S^p\beta$ to be β positively stabilized once at an innermost point p . That is: insert σ_n at the point p on the diagram.

Proposition 4.3.2. *$\kappa(\beta)$ is not a transverse invariant.*

Proof. This is due to the fact that the chain map corresponding to positive stabilization is not filtered (see Proposition 4.3.3). We have a concrete example: consider the braid $B(0, 0)$ from Proposition 4.0.2. By computation, $\kappa(B(0, 0)) = 2$ and $\kappa(S^p B(0, 0)) = 4$ for all choices of innermost points p . □

We note here that we can define a transverse invariant using κ , though it is not clear how to compute it unless the transverse link is known to be represented by a braid with $\kappa = 2$.

Definition 4.3.1. For an n -braid β , define $\kappa_{\min}(\beta)$ to be the minimum $\kappa(K)$ over all transverse representatives K of β . It is a transverse invariant.

We can give bounds on the behavior of κ under positive stabilization:

Proposition 4.3.3. $\kappa(\beta) \leq \kappa(S^p\beta) \leq \kappa(\beta) + 2$.

$$\begin{array}{ccc}
 \phi: \begin{array}{c} \text{---} \\ \diagup \quad \diagdown \\ \times \\ \diagdown \quad \diagup \\ \text{---} \end{array} \longrightarrow 0 & \rho: \begin{array}{c} | \\ v_+ \\ | \end{array} \longrightarrow \begin{array}{c} | \\ v_+ \quad v_- \\ \times \\ | \end{array} + \begin{array}{c} | \\ v_- \quad v_+ \\ \times \\ | \end{array} \\
 \begin{array}{c} | \\ v_- \\ \times \\ | \end{array} \longrightarrow \begin{array}{c} | \\ | \end{array} & \begin{array}{c} | \\ v_- \\ | \end{array} \longrightarrow \begin{array}{c} | \\ v_- \quad v_- \\ \times \\ | \end{array} \\
 \begin{array}{c} | \\ v_+ \\ \times \\ | \end{array} \longrightarrow 0 &
 \end{array}$$

Figure 4.1: Chain maps for positive stabilization

Proof. $S^p\beta$ has a positive crossing at p , and for an n -strand braid β we refer to this crossing as $\sigma_{n,p}$. Suppose that $\sigma_{n,p}$ appears last in the crossing ordering. We show the first inequality. As described in [11], there is a chain map $\phi: CKh(S^p\beta) \rightarrow CKh(\beta)$ whose kernel contains all elements in resolutions of $S^p\beta$ where $\sigma_{n,p}$ is 1-resolved and satisfying

$$\phi(z \otimes v_-) = z$$

$$\phi(z \otimes v_+) = 0$$

for elements in resolutions where $\sigma_{n,p}$ is 0-resolved (see Figure 4.1). Consider an element $y \in CKh(S^p\beta)$ realizing $\kappa(S^p\beta)$. The element y takes the form $z_1 \otimes v_- + z_2 \otimes v_+ + z_3$. So

$$d(\phi(y)) = d(z_1) = \phi(dy) = \phi(\psi(S^p\beta)) = \psi(\beta)$$

Hence z_1 kills $\psi(\beta)$, and so we have

$$\begin{aligned}\kappa(S^p\beta) &= \max k(z_1 \otimes v_-, z_2 \otimes v_+, z_3) + n + 1 \\ &\geq k(z_1 \otimes v_-) + n + 1 = k(z_1) + n \\ &\geq \kappa(\beta)\end{aligned}$$

As described in [11] (see also [52]), there is a chain map $\rho: CKh(\beta) \rightarrow CKh(S^p\beta)$ satisfying $\rho(\psi(\beta)) = \psi(S^p\beta)$. It is given by

$$\begin{aligned}\rho(v_-) &= v_- \otimes v_- \\ \rho(v_+) &= v_+ \otimes v_- + v_- \otimes v_+\end{aligned}$$

Hence ρ can either decrease k -grading by one or increase it by one, depending on whether the circles in question are trivial or non-trivial. Now, suppose we have an element $y \in CKh(\beta)$ realizing $\kappa(\beta)$: then $\rho(y)$ kills $\psi(S^p\beta)$. The k -grading of $\rho(y)$ is at most $\kappa(\beta) - n + 1$. Stabilization increases strand number by one, so $\kappa(S^p\beta)$ could at most be

$$\kappa(\beta) - n + 1 + n + 1 = \kappa(\beta) + 2.$$

□

4.3.4 Other properties and consequences

Propositions 4.3.1 and 4.3.3 immediately give us bounds for κ of braids related by exchange moves and positive flypes:

Proposition 4.3.4. *If two braids σ and β are related by a single exchange move or a single positive flype, then $|\kappa(\sigma) - \kappa(\beta)| \leq 2$.*

Proof. Exchange moves and positive flypes can both be expressed as a composition of braid isotopies, one single positive stabilization, and one single positive destabilization (see for instance [13], [41]). □

Proposition 4.3.5. *Suppose a closed n -braid β can be represented by a braid word containing a factor of σ_i^{-1} but no σ_i 's for some $i = 1, \dots, n-1$. Then $\kappa(\beta) = 2$.*

Proof. The argument we give here is very similar to arguments found in [52]. Consider the resolution formed from taking the 0-resolution of one of the σ_i^{-1} 's, the 1-resolution for all other negative crossings, and the 0-resolution for all positive crossings. We claim that assigning each circle in this resolution v_- yields an element y with $dy = \psi$ and $k(y) = -n+2$. The differential d on y is the sum of all maps with y as their initial end. By our choice of resolution, any map corresponding to a merge map sends y to 0. Hence d is a sum of split maps. Topologically, the only split maps that can start from this resolution are in the i 'th column; however, there are only negative crossings in this column, and at this resolution they are all 1-resolved except for the one that is 0-resolved. So the only contributor to dy is the map resolving that crossing, sending y to $\psi(\beta)$. \square

Corollary 4.3.6. *If an n -braid σ is not right-veering, then $\kappa(\sigma) = 2$.*

Proof. By Proposition 3.1 of [7] and Proposition 6.2.7 of [16], σ is conjugate to a braid that can be represented by a word containing at least a factor of σ_i^{-1} but no σ_i 's for some $i = 1, \dots, n$. The result follows by Proposition 4.3.5. \square

For a braid $\beta \in B_n$ we denote its mirror as $m(\beta) \in B_n$.

Corollary 4.3.7. *If $\kappa(\sigma) \neq 2$ and $\kappa(m(\sigma)) \neq 2$, then $\sigma = 1 \in B_n$.*

Proof. The proof is similar to that of Corollary 1 of [7]. By Corollary 4.3.6, σ and $m(\sigma)$ are right-veering and hence σ is also left-veering. By Lemma 3.1 of [7], σ is the identity braid. \square

This implies that κ solves the word problem. Indeed, the solution is faster than that of [7], since it is only necessary to check if Plamenevskaya's invariant vanishes by the E^3 page of the spectral sequence from annular Khovanov homology to Khovanov homology.

κ provides an obstruction to negative destabilization (Proposition 4.3.1). It can also provide an obstruction to positive destabilization for a braid in the case that $\kappa \neq 2$ for its mirror. Corollary 4.3.7 implies that it cannot provide an obstruction to destabilization in

general. One might hope to show that $\kappa \neq 2$ for a braid and $\kappa \neq 2$ for its mirror, implying that the braid is neither negatively destabilizable nor positively destabilizable. However, Corollary 4.3.7 shows that if this is the case, the braid is trivial.

We end this section with a remark on spectral sequences. For any annular link L , there is a spectral sequence whose E^0 page is the annular Khovanov complex of L and whose E^1 page is, as a group, the annular Khovanov homology of L . Since there are no differentials that drop the k -grading by one, the E^2 page is identical to the E^1 page. Therefore the first page at which the spectral sequence could collapse is E^3 . The following proposition provides a counterexample to Conjecture 4.2 from [30].

Proposition 4.3.8. *The spectral sequence from annular Khovanov homology to Khovanov homology does not always collapse at the E^3 page.*

Proof. We consider the braid $A(0,0)$ from Proposition 4.0.2. The distinguished element $\psi(A(0,0))$ lives in homological grading 4 (before any final shifts) and has k grading -4 . Recall that $\psi(A(0,0))$ is unique in the lowest k -grading. By $E_{d,m}^r$ we mean the r 'th page of the spectral sequence at homological grading d and k -grading m .

Following [31] (recall: the differentials on CKh increase homological grading),

$$\begin{aligned} E_{4,-4}^3 &= \frac{\{x \in \mathcal{F}_{-4}CKh_4 \mid dx \in \mathcal{F}_{-7}CKH_5\}}{\mathcal{F}_{-5}CKh_4 + d(\mathcal{F}_{-2}CKh_3)} = \frac{\{x \in \mathcal{F}_{-4}CKh_4 \mid dx = 0\}}{d(\mathcal{F}_{-2}CKh_3)} \\ &= \frac{\text{span}\{\psi(A(0,0))\}}{d(\mathcal{F}_{-2}CKh_3)} = [\psi(A(0,0))] \neq 0 \end{aligned}$$

since $\kappa(A(0,0)) \neq 2$. However, $[\psi(A(0,0))] = 0 \in Kh_4(A)$, and hence $Kh_4(A(0,0)) \neq \bigoplus_{k=-4}^4 E_{4,k}^3$.

□

Precisely the same argument yields a more general statement:

Proposition 4.3.9. *Given a braid β , the length of the spectral sequence from $\text{AKh}(\bar{\beta})$ to $\text{Kh}(\bar{\beta})$ is bounded below by $\kappa(\beta)$.*

4.4 Invariants in reduced Khovanov homology

It is implicit in the proof of Proposition 4.3.3 that κ increases under positive stabilization at p precisely if every element which realizes κ has a canonical summand in which p lies on a trivial v_+ -labeled circle. This situation cannot occur in (one version of) reduced Khovanov homology, and so one might hope that a “reduced κ ” is an invariant of transverse links. That’s not quite the case – the eager reader may skip to the examples at the end of this section – but the reduced invariants are interesting in their own right.

In this section let p be a non-double point on an n -strand annular braid diagram \mathcal{D} of $\bar{\beta}$. For convenience, we will assume that the last tensor factor of each generator of $\text{CKh}(\mathcal{D})$ corresponds to the component containing p . The k -grading on $\text{CKh}(\mathcal{D})$ induces a k -grading on each variant of reduced Khovanov homology. On the subcomplex $\widetilde{\text{CKh}}_p(\mathcal{D})$ this is simply the restriction. We define the k -grading on $\underline{\text{CKh}}_p(\mathcal{D})$ via canonical representatives: if \underline{y} is the canonical representative of $y \in \underline{\text{CKh}}_p(\mathcal{D})$, then $k(\underline{y}) = k(y)$. However, the isomorphism between the two variants is not in general k -filtered. Thus we will distinguish their homologies as the *reduced homology* $\widetilde{Kh}_p(\mathcal{D})$ and the *reduced quotient homology* $\underline{Kh}_p(\mathcal{D})$. We write $\widetilde{\mathcal{F}}_i$ and $\underline{\mathcal{F}}_i$ for the i th filtered levels of $\widetilde{\text{CKh}}_p(\mathcal{D})$ and $\underline{\text{CKh}}_p(\mathcal{D})$ respectively.

Each complex supports a variant of the transverse element $\psi(\mathcal{D})$. The cycle corresponding to $\psi(\mathcal{D})$ is also a cycle in the subcomplex $\widetilde{\text{CKh}}_p(\mathcal{D})$ for any p . When we wish to emphasize that we are considering $\psi(\mathcal{D})$ as an element of the subcomplex, we will write it as $\widetilde{\psi}_p(\mathcal{D})$. Plamenevskaya defines the reduced quotient invariant $\underline{\psi}_p(\mathcal{D})$ to be the image of the chain $v_- \otimes \cdots \otimes v_- \otimes v_+$ in $\underline{\text{CKh}}_p(\mathcal{D})$. Both $\widetilde{\psi}_p$ and $\underline{\psi}_p$ are invariant under braid conjugation and stabilization away from p in the same sense (and with the same proofs) as ψ . Both cycles have the lowest k -grading in their respective complexes, but $\underline{\psi}_p$ does not necessarily generate that lowest level.

As these constructions depend on a choice of p on a particular diagram for a link, we will not write “ $\widetilde{\psi}_p(\bar{\beta})$ ” or “ $\underline{\psi}_p(\bar{\beta})$ ”.

Definition 4.4.1. Let $\beta \in B_n$, let \mathcal{D} be an annular diagram for $\bar{\beta}$, and let $p \in \mathcal{D}$. If $\widetilde{\psi}_p(\mathcal{D})$

is a boundary in $\widetilde{\text{CKh}}_p(\mathcal{D})$, define

$$\tilde{\kappa}_p(\mathcal{D}) = n + \min\{i : [\tilde{\psi}_p(\mathcal{D})] = 0 \in H_*(\tilde{\mathcal{F}}_i(\mathcal{D}))\}.$$

If $\tilde{\psi}_p(\mathcal{D})$ is not a boundary, then define $\tilde{\kappa}_p(\mathcal{D}) = \infty$. If $\psi_p(\mathcal{D})$ is a boundary in $\underline{\text{CKh}}_p(\mathcal{D})$, define

$$\underline{\kappa}_p(\mathcal{D}) = n + \min\{i : [\underline{\psi}_p(\mathcal{D})] = 0 \in H_*(\underline{\mathcal{F}}_i(\mathcal{D}))\}.$$

If $\underline{\psi}_p(\mathcal{D})$ is not a boundary, then define $\underline{\kappa}_p(\mathcal{D}) = \infty$.

The arguments of Section 4.2 show that $\tilde{\kappa}_p(\mathcal{D})$ and $\underline{\kappa}_p(\mathcal{D})$ are invariant under positive stabilization away from p and conjugations that do not cross p .

Lemma 4.4.1. *For a fixed diagram \mathcal{D} , either $\kappa(\mathcal{D})$, $\tilde{\kappa}_p(\mathcal{D})$, and $\underline{\kappa}_p(\mathcal{D})$ are all finite or all infinite. In the finite case, $\kappa(\mathcal{D}) \leq \tilde{\kappa}_p(\mathcal{D}) \leq \underline{\kappa}_p(\mathcal{D}) \leq \tilde{\kappa}_p(\mathcal{D}) + 2$.*

Proof. There is a short exact sequence of complexes

$$0 \rightarrow \widetilde{\text{CKh}}_p(\mathcal{D}) \xrightarrow{i_*} \text{CKh}(\mathcal{D}) \xrightarrow{\pi} \underline{\text{CKh}}_p(\mathcal{D}) \rightarrow 0$$

where i is the inclusion and π is the projection to the quotient. The induced map on homology i_* carries $[\tilde{\psi}_p(\mathcal{D})]$ to $[\psi(\mathcal{D})]$, so if $[\psi(\mathcal{D})] \neq 0$ then $[\tilde{\psi}_p(\mathcal{D})] \neq 0$. If i_* is injective, then $[\tilde{\psi}_p(\mathcal{D})] \neq 0$ implies that $[\psi(\mathcal{D})] \neq 0$. To show that i_* is injective, we repeat Shumakovitch's argument [60] in our notation. Let $\nu: \text{CKh}(\mathcal{D}) \rightarrow \text{CKh}(\mathcal{D})$ be the chain map defined on V by the rule $\nu(v_+) = 0$ and $\nu(v_-) = v_+$ and extended to tensor powers by the Leibniz rule. Note that x_p defines a map $x'_p: \underline{\text{CKh}}_p(\mathcal{D}) \rightarrow \text{CKh}(\mathcal{D})$ by applying x_p to canonical representatives. Let $\underline{c} \in \underline{\text{CKh}}_p(\mathcal{D})$ with canonical representative c . Then $(\nu \circ x'_p)(\underline{c}) = (\nu \circ x_p)(c)$, in which the only term with a v_+ label at p is exactly c . We conclude that $\pi \circ \nu \circ x'_p$ is the identity map, and therefore the short exact sequence splits. Thus i_* is injective.

The first piece of the inequality follows immediately from the fact that $\widetilde{\text{CKh}}_p(\mathcal{D})$ is a subcomplex of $\text{CKh}(\mathcal{D})$. For the next part, suppose that \underline{z} realizes $\underline{\kappa}_p(\mathcal{D})$. Then $d(x_p z) = \psi(\mathcal{D})$ and $k(x_p z) \leq k(\underline{z})$, so $\tilde{\kappa}_p(\mathcal{D}) \leq \underline{\kappa}_p(\mathcal{D})$. On the other hand, suppose that y realizes $\tilde{\kappa}_p(\mathcal{D})$; every canonical summand of y has a v_- at p . Let y^+ be the element obtained from

y by changing those v_- 's to v_+ 's. Clearly $x_p d(\underline{y}^+) = \psi(\mathcal{D})$, so

$$dy^+ = \underline{\psi}_p(\mathcal{D}) + \text{terms with } v_- \text{ at } p.$$

Therefore $d\underline{y}^+ = \underline{\psi}_p(\mathcal{D})$ and $\underline{\kappa}_p(\mathcal{D}) \leq k(y^+) + n \leq k(y) + 2 + n = \tilde{\kappa}_p(\mathcal{D}) + 2$. (This also shows that $\tilde{\kappa}_p(\mathcal{D})$ is finite if and only if $\underline{\kappa}_p(\mathcal{D})$ is finite.) \square

The reduced invariants are stable under positive stabilization at p in the following sense: let p' be a point on the same arc as p . For each reduced complex, the positive stabilization map is filtered and preserves Plamanevskaya's invariant, so Lemma 4.2.1 implies that the appropriate version of κ does not change. But after this operation the image of p is not an innermost point. We instead study $\vec{S}^{p'}$, the operation of stabilizing at p' and then moving the basepoint to some point q on the new innermost strand.

Proposition 4.4.2. *Let \mathcal{D} be a diagram of $\bar{\beta}$. Then $\tilde{\kappa}_q(\vec{S}^{p'}\mathcal{D}) \leq \tilde{\kappa}_p(\mathcal{D})$ and $\underline{\kappa}_q(\vec{S}^{p'}\mathcal{D}) \leq \underline{\kappa}_p(\mathcal{D}) + 2$.*

Proof. The first inequality follows from Lemma 4.2.1 once one makes the observation that the positive stabilization map carries $\widetilde{\text{CKh}}_p(\mathcal{D})$ to a subcomplex of $\widetilde{\text{CKh}}_q(\vec{S}^{p'}\mathcal{D})$ and carries $\tilde{\psi}_p(\mathcal{D})$ to $\tilde{\psi}_q(\mathcal{D})$.

Suppose that \underline{z} realizes $\underline{\kappa}_p(\mathcal{D})$. Let q be a point on the innermost strand of $S^{p'}\mathcal{D}$. Recall that there is a map ρ on the Khovanov complex induced by positive stabilization. This map descends to a map $\rho: \underline{\text{CKh}}_p(\mathcal{D}) \rightarrow \underline{\text{CKh}}_p(S^{p'}\mathcal{D})$ which sends \underline{z} to a sum of generators with v_- at q and v_+ at p . Let $\underline{z}' \in \underline{\text{CKh}}_q(\vec{S}^{p'}\mathcal{D})$ be the element whose canonical representative z' is obtained from that of $\rho(\underline{z})$ by swapping these labels. Note that $dx_q z' = \rho(\psi(\mathcal{D})) = x_q dz'$, so $d\underline{z}' = \underline{\psi}_q(\mathcal{D})$. Clearly $k(\underline{z}') \leq k(\underline{z}) + 1$. The second inequality follows after taking into account that the operation $S^{p'}$ increases braid index by one. \square

It is interesting to consider the sharpness of these inequalities using annular Khovanov homology. The map x_p is filtered and therefore induces a map on $\text{AKh}(\mathcal{D}) = \bigoplus \mathcal{F}_i / \mathcal{F}_{i-1}$, the annular Khovanov homology of \mathcal{D} .

Let p, p', z , and z' be as in the previous proof. The point q lies on a non-trivial circle in every resolution of $S^{p'}\mathcal{D}$, so $k(z') > k(S^{p'}z) = k(z)$ precisely if p lies on a trivial circle in

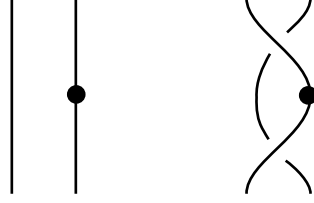


Figure 4.2: The result of the operation \vec{C}_p on two strands.

some canonical summand of z . Equivalently, $k(z') = k(z)$ precisely if p lies on a non-trivial circle in every canonical summand of z . Therefore $\underline{\kappa}_p(\mathcal{D}) = \underline{\kappa}_q(\vec{S}^{p'}\mathcal{D})$ if and only if some z realizes $\underline{\kappa}_p(\mathcal{D})$ and p lies on a non-trivial circle in every canonical summand of z . Write $\langle z \rangle$ for the image of z in $\text{AKh}(\mathcal{D})$. Then $\underline{\kappa}_p(\mathcal{D}) = \underline{\kappa}_q(\vec{S}^{p'}\mathcal{D})$ if and only if $\langle z \rangle \in \ker(x_p)$ for some z which realizes $\underline{\kappa}_p(\mathcal{D})$.

While $\underline{\kappa}_p$ is not preserved under stabilization, it is preserved under a certain sort of conjugation over p . Denote by C_p the operation of performing a braidlike Reidemeister 2 move over p . (In terms of braid words, this inserts $\sigma_{n-1}\sigma_{n-1}^{-1}$ or $\sigma_{n-1}^{-1}\sigma_{n-1}$.) Denote by \vec{C}_p the operation C_p followed by moving the basepoint to the innermost strand at q . See Figure 4.2. The Reidemeister 2 map induces a filtered map $\text{CKh}_p(\mathcal{D}) \rightarrow \text{CKh}_q(\vec{C}_p\mathcal{D})$ which carries ψ to ψ .

Proposition 4.4.3. $\underline{\kappa}_p(\mathcal{D}) = \underline{\kappa}_q(\vec{C}_p\mathcal{D})$.

To dash any hope that $\underline{\kappa}_p$ or $\tilde{\kappa}_p$ might be transverse invariants, we note that both invariants depend on p . For $\underline{\kappa}_p$ this is true even for negative stabilizations.

Example 3. Let $\beta = \sigma_1\sigma_2^{-1} \in B_3$. Certainly ψ is null-homologous and $\kappa = \tilde{\kappa}_p = 2$ for any p . Let p_1 and p_2 be points on the first and second strands of the braid. Then

$$\underline{\kappa}_{p_1} = 2$$

$$\underline{\kappa}_{p_2} = 4$$

For a meatier example, we revisit the transversely non-simple family using the previously advertised computer program.

Example 4. Recall that Ng and Kandhawit define two infinite families of braids $A(a, b)$ and $B(a, b)$ so that, for any $a, b \in \mathbb{Z}_{\geq 0}$, the closures of $A(a, b)$ and $B(a, b)$ have the same

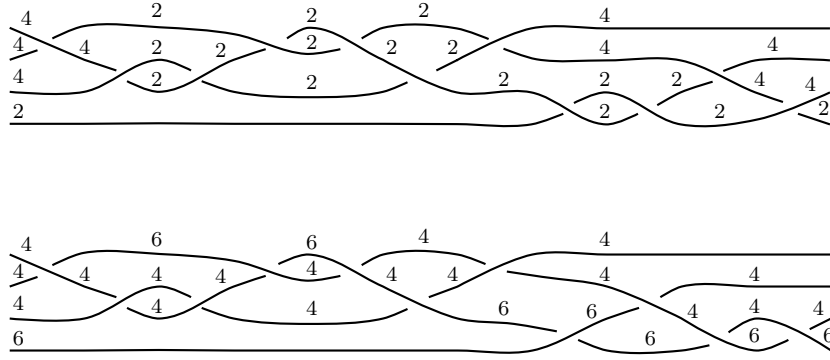


Figure 4.3: Values of $\underline{\kappa}_p$ and $\tilde{\kappa}_p$ may depend on p . The top braid is B_0 and the bottom braid is A_0 . The number above each arc represents a value of $\underline{\kappa}_p$ (for A_0) or $\tilde{\kappa}_p$ (for B_0) when p is placed on that arc.

topological knot type and self-linking number but are not transversely isotopic. Write A_0 and B_0 for $A(0, 0)$ and $B(0, 0)$. We have already seen that $\kappa(A_0) = 4$ and $\kappa(B_0) = 2$. For any $p \in \bar{A}_0$ we have $\tilde{\kappa}_p(A_0) = 4$ and $\underline{\kappa}_p(B_0) = 4$. On the other hand, $\underline{\kappa}_p(A_0)$ and $\tilde{\kappa}_p(B_0)$ depend on p . See Figure 4.3.

It is straightforward to check that the two candidates for “reduced annular Khovanov homology” are not isomorphic (for example with the closed 2-braid $\overline{\sigma_1}$). This fact is not mentioned elsewhere in the literature. In addition, Shumakovitch’s map ν (see Lemma 4.4.1) is not a chain map on the annular complex as it does not commute with the differential. These calculations show that the difference between the two versions is significant, and that the two reductions might provide different information.

Bibliography

- [1] J. W. Alexander. A lemma on systems of knotted curves. *Proceedings of the Natural Academy of Sciences*, 9, 1923.
- [2] 4th century BCE Aristote. *Aristotle On the Heavens*. Harvard University Press, 1939.
- [3] Emil Artin. Theory of braids. *Annals of Mathematics*, 48(1):101–126.
- [4] Marta Asaeda, Józef Przytycki, and Adam Sikora. Categorification of the Kauffman bracket skein module of I -bundles over surfaces. *Contemporary Mathematics*, 416:1–8, 2006.
- [5] John Baldwin and David Shea Vela-Vick. A refinement of the contact invariant in heegaard floer theory. *In preparation*.
- [6] John A. Baldwin. On the spectral sequence from Khovanov homology to Heegaard Floer homology. *International Mathematics Research Notices*, (15):3426–3470, 2011.
- [7] John A. Baldwin and J. Elisenda Grigsby. Categorified invariants and the braid group. *Proc. Amer. Math. Soc.*, pages 2801–2814, 2015.
- [8] John A. Baldwin, Matthew Hedden, and Andrew Lobb. On the functoriality of Khovanov-Floer theories. *arxiv preprint arxiv:1509.04691*, 2015.
- [9] John A. Baldwin and Olga Plamenevskaya. Khovanov homology, open books, and tight contact structures. *Adv. Math.*, 224(6):2544–2582, 2010.
- [10] Dror Bar-Natan. On khovanov’s categorification of the jones polynomial. *Algebraic and Geometric Topology*, 2(16):337–370, 2002.
- [11] Dror Bar-Natan. Khovanov’s homology for tangles and cobordisms. *Geometry & Topology*, 9(3):1443–1499, 2005.
- [12] Joan S. Birman and William M. Menasco. Stabilization in the braid groups II: Transversal simplicity of knots. *Geometric Topology*, (10):1425–1452, 2006.
- [13] Joan S. Birman and Nancy C. Wrinkle. On transversally simple knots. *Journal of Differential Geometry*, 55(2):325–354, 2000.
- [14] 7th cent. Brahmagupta. *Classics of Indian mathematics : algebra, with arithmetic and mensuration, from the Sanskrit of Brahmagupta and Bhāskara*. Sharada Pub. House, 2005.

- [15] Markus Bröcher. Bowline knot, 2008. Available at https://commons.wikimedia.org/wiki/File:Palstek_innen.jpg, accessed March 26, 2016.
- [16] Patrick Dehornoy, Ivan Dynnikov, Dale Rolfsen, and Bert Wiest. Why are braids orderable?, volume 14 of Panoramas et Synthèses [Panoramas and Synthèses]. *Société Mathématique de France, Paris*, 2002.
- [17] Yakov Eliashberg and M-L Yau. Vanishing of the contact homology of overtwisted 3-manifolds. *Bull. Inst. Math. Acad. Sin.*, (1):211–229, 2006.
- [18] John B. Etnyre and Ko Honda. Cabling and transversal simplicity. *Annals of Mathematics*, 162(2):253–268, 2005.
- [19] Pearson Scott Foresman. Bowline, 2007. Available at [https://commons.wikimedia.org/wiki/File:Bowline_\(PSF\).jpg](https://commons.wikimedia.org/wiki/File:Bowline_(PSF).jpg), accessed March 26, 2016.
- [20] Dmitry Fuchs and Serge Tabachnikov. Invariants of transverse and legendrian knots in the standard contact space. *Topology*, 36(5):1025–1053, 1997.
- [21] F. A. Garside. The braid group and other groups. *The Quarterly Journal of Mathematics*, 20(1):235–254, 1969.
- [22] Paolo Ghiggini, Ko Honda, and Jeremy Van Horn-Morris. The vanishing of the contact invariant in the presence of torsion. *arXiv preprint arXiv:0706.1602*, 2008.
- [23] Robert E. Gompf and András Stipsicz. *Four-manifolds and Kirby calculus*. American Mathematical Society, 1999.
- [24] John W. Gray. Some global properties of contact structures. *Annals of Mathematics*, 1959.
- [25] J. Elisenda Grigsby and Yi Ni. Sutured Khovanov homology distinguishes braids from other tangles. *Math. Res. Letters*, (6):1263–1275, 2014.
- [26] J. Elisenda Grigsby and Stephan M. Wehrli. On gradings in Khovanov homology and sutured Floer homology. *Topology and geometry in dimension three*, 560:111–128, 2011.
- [27] Mikhail Gromov. Pseudoholomorphic curves in symplectic manifolds. *Inventiones Mathematicae*, 82:307–347, 1985.
- [28] Diana Hubbard. On sutured Khovanov homology and axis-preserving mutations. *arXiv preprint arXiv:1505.03091*, 2015.
- [29] Diana Hubbard and Adam Saltz. An annular refinement of the transverse invariant in Khovanov homology. *Algebraic and Geometric Topology, accepted*, 2016.
- [30] Hilary Hunt, Hannah Keese, Anthony Licata, and Scott Morrison. Computing annular Khovanov homology. *arXiv preprint arXiv:1505.04484*, 2015.
- [31] Michael Hutchings. Introduction to spectral sequences. 2011. Available at <https://math.berkeley.edu/~hutching/teach/215b-2011/ss.pdf>.
- [32] Magnus Jacobsson. An invariant of link cobordisms from khovanov homology. *Algebraic and Geometry Topology*, 4, 2004.

- [33] Tirasan Khandhawit and Lenhard Ng. A family of transversely nonsimple knots. *Algebraic & Geometric Topology*, 10(1):293–314, 2010.
- [34] Mikhail Khovanov. A categorification of the Jones polynomial. *Duke Math J.*, 101(3), 2000.
- [35] Mikhail Khovanov. Patterns in knot cohomology I. *Experiment. Math.*, 12(3):365–374, 2003.
- [36] Mikhail Khovanov. An invariant of tangle cobordisms. *Trans. Amer. Math. Soc.*, (358):315–327, 2006.
- [37] Cagatay Kutluhan, Gordana Matić, Jeremy Van Horn-Morris, and Andy Wand. Filtering the Heegaard Floer contact invariant. *arXiv preprint arXiv:1603.02673*, 2016.
- [38] Jenko Latschev and Chris Wendl with Michael Hutchings. Algebraic torsion in contact manifolds. *Geom. Funct. Anal.*, 21:1144–1195, 2011.
- [39] Y-J. Lee. Heegaard splittings and Seiberg-Witten monopoles. In Hans U. Boden, Ian Hambleton, Andrew J. Nicas, and B. Doug Park, editors, *Geometry and topology of manifolds*, volume 47 of *Fields Institute Communications*, pages 173–202. AMS and Fields Institute, 2005.
- [40] Robert Lipshitz. A cylindrical reformulation of heegaard floer homology. *Geometry & Topology*, 2006.
- [41] Robert Lipshitz, Lenhard Ng, and Sucharit Sarkar. On transverse invariants from Khovanov homology. *arXiv preprint arXiv:1303.6371*, 2013.
- [42] Andrey Markov. Über die freie aquivalenz der geschlossenen zöpfe. *Recueil Mathématique De La Socit Mathématique De Moscou*, 1935.
- [43] John McCleary. *A User's Guide to Spectral Sequences*, volume 58 of *Cambridge Studies in Advanced Mathematics*. Cambridge University Press, second edition, 2000.
- [44] John Milnor. *Morse Theory*. Princeton University Press, 1963.
- [45] S. Yu. Orevkov and V. V. Shevchishin. Markov theorem for transversal links. *J. of Knot Theory and Ramifications*, 12:905–913, 2003.
- [46] Burak Ozbagci and Andrs Stipsicz. *Surgery on Contact 3-Manifolds and Stein Structures*. Bolyai Society Mathematical Studies, 2004.
- [47] Peter Ozsváth and Zoltán Szabó. Holomorphic disks and three-manifold invariants: properties and applications. *Ann. of Math. (2)*, 159(3):1159–1245, 2004.
- [48] Peter Ozsváth and Zoltán Szabó. Holomorphic disks and topological invariants for closed three-manifolds. *Ann. of Math. (2)*, 159(3):1027–1158, 2004.
- [49] Peter Ozsváth and Zoltán Szabó. Heegaard Floer homology and contact structures. *Duke Math. J.*, 129(1):39–61, 2005.
- [50] Peter Ozsváth and Zoltán Szabó. On the Heegaard Floer homology of branched double covers. *Adv. Math.*, pages 1–33, 2005.

- [51] Peter Ozsváth and Zoltán Szabó. Holomorphic triangles and invariants for smooth four-manifolds. *Adv. Math.*, 202(2):236–400, 2006.
- [52] Olga Plamenevskaya. Transverse knots and Khovanov homology. *Math. Res. Lett.*, (4):571–586, 2006.
- [53] Jacob Rasmussen and Liam Watson. Floer homology and low-dimensional topology.
- [54] Lawrence Roberts. Notes on the Heegaard-Floer link surgery spectral sequence. *arxiv preprint arxiv:0808.2817*, 2008.
- [55] Lawrence Roberts. On knot Floer homology in double branched covers. *Geometry & Topology*, 17:413–467, 2013.
- [56] Dale Rolfsen. *Knots and Links*. Publish or Perish, 1976.
- [57] Adam Saltz. Branched diagrams and the Ozsváth-Szabó spectral sequence. *arxiv preprint arXiv:1510.02819*, 2015.
- [58] Sucharit Sarkar. Maslov index formulas for Whitney n -gons. *J. Symplectic Geom.*, 9(2):251 – 270, 2011.
- [59] Cotton Seed. Computations of szabó’s geometric spectral sequence in Khovanov homology. *arxiv preprint arxiv:1110.0735*, 2011.
- [60] Alexander Shumakovitch. Torsion of the Khovanov homology. *arxiv preprint arxiv:0405474*, 2004.
- [61] Zoltán Szabó. A geometric spectral sequence from Khovanov homology. *arxiv preprint arxiv:1010.4252*, 2013.
- [62] Nancy Wrinkle. *The Markov theorem for transverse knots*. PhD thesis, Columbia University, 2002.